Tracking the kinetics and phenotype of spike epitope-specific CD4 T cell immunity in the context of SARS-CoV-2 infection and vaccination

Jennifer Juno (jennifer.juno@unimelb.edu.au)
University of Melbourne at the Peter Doherty Institute for Infection and Immunity
https://orcid.org/0000-0002-9072-1017

Kathleen Wragg
The University of Melbourne

Wen Shi Lee
The University of Melbourne

Thakshila Amarasena
The University of Melbourne

Arnold Reynaldi
UNSW Australia

Marios Koutsakos
University of Melbourne

Penny Konstandopoulos
The University of Melbourne

Kirsty Field
The University of Melbourne

Robyn Esterbauer
University of Melbourne https://orcid.org/0000-0002-7091-0048

Hyon-Xhi Tan
University of Melbourne

Helen Kent
The University of Melbourne

Miles Davenport
UNSW Sydney https://orcid.org/0000-0002-4751-1831

Adam Wheatley
University of Melbourne https://orcid.org/0000-0002-5593-9387

Stephen Kent
The University of Melbourne https://orcid.org/0000-0002-8539-4891

Article

Keywords: SARS-CoV-2, CD4+ T cells, vaccination

Posted Date: October 19th, 2021

DOI: https://doi.org/10.21203/rs.3.rs-957030/v1

Version of Record: A version of this preprint was published at Nature Immunology on March 21st, 2022.
See the published version at https://doi.org/10.1038/s41590-022-01175-5.

Tracking the kinetics and phenotype of spike epitope-specific CD4 T cell immunity in the context of SARS-CoV-2 infection and vaccination

Wragg KM[1*], Lee WS[1*], Amarasena T[1], Reynaldi A[2], Koutsakos M[1], Konstandopoulos P[1], Field KR[1], Esterbauer R[1], Tan HX, Kent HE[1], Davenport MP[2], Wheatley AK[1], Kent SJ[1,3], Juno JA[1]

[*]Contributed equally

[1]Department of Microbiology and Immunology, University of Melbourne at the Peter Doherty Institute for Infection and Immunity, Melbourne Australia

[2]Kirby Institute, University of New South Wales, Sydney Australia

[3]Melbourne Sexual Health Centre and Department of Infectious Diseases, Alfred Hospital and Central Clinical School, Monash University, Melbourne, Victoria, Australia

Correspondence:

Dr. Jennifer Juno, jennifer.juno@unimelb.edu.au

Dr. Stephen Kent, skent@unimelb.edu.au

Abstract:

$CD4^+$ T cells play a critical role in the immune response to viral infection. SARS-CoV-2 infection and vaccination elicit strong $CD4^+$ T cell responses to the viral spike protein, including circulating T follicular helper (cTFH) cells that correlate with the development of neutralising antibodies. Here we use a novel HLA-DRB1*15:01/S_{751} tetramer to precisely track spike-specific $CD4^+$ T cells following recovery from mild/moderate COVID-19, or after vaccination with spike-encoding vaccines. SARS-CoV-2 infection induces robust S_{751}-specific responses with both $CXCR5^-$ and cTFH phenotypes that are maintained for at least 12 months in a stable, CXCR3-biased, central memory pool. Vaccination of immunologically naïve subjects similarly drives expansion of S_{751}-specific T cells with a highly restricted TCR repertoire comprised of both public and private clonotypes. Vaccination of convalescent individuals drives recall of $CD4^+$ T cell clones established during infection, which are shared between the $CXCR5^-$ and cTFH compartments. This recall response is evident 5 days after antigen exposure and includes a population of spike-specific cTFH that persist in the periphery after losing expression of PD-1. Overall this study demonstrates the generation of a stable pool of cTFH and memory $CD4^+$ T cells that can be recalled upon spike antigen re-exposure, which may play an important role in long-term protection against SARS-CoV-2 infection.

Introduction:

$CD4^+$ T cells coordinate and support multiple aspects of adaptive immunity, including B cell activation and maturation, $CD8^+$ T cell responses, and production of antiviral cytokines. Studies have demonstrated that SARS-CoV-2 infection induces robust $CD4^+$ T cell responses[1,2] that persist for at least 8 months post-infection[3-6]. These responses, directed toward both the spike and other viral proteins, have been implicated in the control of SARS-CoV-2 infection through multiple mechanisms. Total $CD4^+$ and $CD8^+$ responses to spike, membrane and nucleocapsid proteins have been associated with a reduction in COVID-19 disease severity[5], suggesting a potential contribution of T cells to control of viral pathogenesis. Additionally, many studies have investigated the capacity of spike-specific $CD4^+$ T follicular helper (TFH) cells to support B cell maturation and neutralising antibody production following SARS-CoV-2 infection or vaccination[7-9]. Evidence suggests that spike-specific circulating TFH (cTFH) are useful correlates of neutralising antibody titres, both after infection[3-6] or following vaccination[10].

Characterisation of the $CD4^+$ T cell response to SARS-CoV-2 therefore affords an opportunity to define the establishment and features of long-term memory responses during a novel viral infection in human cohorts, and in particular, to characterise the maintenance and recall of both $CXCR5^-$ memory T cells (T_{mem}) and cTFH. Studies have indicated that both infection and vaccination primarily elicit central memory $CD4^+$ T cell responses with cTFH, Th1- and/or Th-17-like phenotypes[3,10-12]. Longitudinal follow-up of convalescent cohorts has suggested that spike-specific $CD4^+$ T cells decline in a linear fashion over the course of 8 months[10,13], with some evidence that spike-specific cTFH frequencies are more stable[14]. In the context of primary vaccination, $CD4^+$ T cell responses persist for at least 6 months, with cTFH frequencies peaking 1 month post-vaccination and subsequently declining[15].

Immunisation of COVID-19 convalescent cohorts, particularly after long-term T cell memory has been established, offers an interesting model in which to study immune recall to antigenic challenge. Despite intense interest in the robust neutralising antibody responses elicited by vaccination of convalescent individuals[16], relatively little has been reported on the associated $CD4^+$ T cell responses[10,13,17]. In particular, there is a paucity of data defining the early kinetics and phenotypes of spike-specific $CD4^+$ and cTFH recall.

To date, most data describing $CD4^+$ T cell recognition of SARS-CoV-2 has been derived from stimulation-based assays (activation induced marker (AIM) or cytokine expression) that assess bulk responses to the full-length spike, or specific protein sub-domains[18]. Characterisation of the *ex vivo* activation state or phenotype of these antigen-specific cells can be challenging, however, due to the requirement for *in vitro* stimulation. The development of pMHC tetramers to track epitope-specific T cell responses has facilitated a detailed understanding of the development and maintenance of T cell memory following viral infection, particularly for $CD8^+$ T cells[19]. In contrast, however, epitope-level $CD4^+$ T cell responses during acute viral infections in adults are less well defined, with most data derived from chronic infections such as HIV, HCV, EBV or CMV[20,21]. In the context of SARS-CoV-2, Oberhardt et al recently demonstrated the expansion of $CD4^+$ T cells recognising a single spike epitope following mRNA vaccination[18], but comparable studies following infection are lacking.

Here, we use a novel HLA-DRB1*15:01 tetramer presenting a SARS-CoV-2 spike epitope ($S_{751\text{-}767}$**)** to define the dynamics of memory CD4 and cTFH cells in three contexts: (1) over 15 months of SARS-CoV-2 convalescence, (2) following vaccination of naïve individuals with spike-based vaccines, and (3) during recall of memory responses following vaccination

of previously infected subjects. Notably, we provide fine mapping of the kinetics of epitope-specific memory $CD4^+$ T cells and their decay over the course of 15 months following SARS-CoV-2 infection. Through TCR sequencing, we demonstrate the recall of $CD4^+$ memory and cTFH clones following antigen re-exposure, and track the long-term persistence and phenotype of spike-specific cTFH. These data provide key knowledge of nascent and recalled $CD4^+$ T cell immunity, providing critical insights into biomarkers of effective immunity against SARS-CoV-2.

Results:

*Identification of a prominent, HLA-DRB1*15:-restricted epitope within the SARS-CoV-2 spike*

We[3,22] and others[23-25] have previously screened $CD4^+$ T cell responses among convalescent COVID-19 or vaccinated individuals and identified an immunogenic spike-derived peptide encompassing the sequence NLLLQYGSFCTQLNRAL ($S_{751\text{-}767;}$ termed S_{751} hereafter). Antibody-based blockade of HLA molecules during activation induced marker (AIM) assays suggested that S_{751} peptide presentation occurred through HLA-DR (Supp Fig 1A). HLA-DRB1*15:01 was the only HLA-DR allele shared by the majority of responders to S_{751} (Supp Table 1), and computational analysis of HLA/peptide binding using NetMHCII2.3[26] similarly predicted strong binding (IC_{50} of 12.1nM) between S_{751} and HLA-DRB1*15:01. We therefore generated HLA-DRB1*15:01/ S_{751} tetramers to identify epitope-specific $CD4^+$ T cells.

Tetramer specificity was assessed in HLA-typed individuals prior to and following SARS-CoV-2 vaccination, or following SARS-CoV-2 infection. Staining of cryopreserved PBMC samples with S_{751}-PE tetramers identified a clear population of $CD4^+$ tetramer-binding (TET_{751}^+) T cells in HLA-DRB1*15 subjects after infection (Fig 1A) or vaccination (Fig 1B). In contrast, individuals lacking the HLA-DRB1*15 allele exhibited no or negligible TET_{751}^+ cells following vaccination or infection (Fig1A, B). TET_{751}^+ cells did not bind a HLA-DRB1*15:01 tetramer loaded with an irrelevant peptide, indicating specificity for the S_{751} peptide (Fig 1C). Among both convalescent and vaccinated subjects, TET_{751}^+ cells were predominately $CD45RA^-$, a phenotype consistent with antigen-experienced T cells (Fig 1D). *In vitro* culture of post-vaccine PBMC with S_{751} peptide clearly demonstrated peptide-driven

proliferation of TET_{751}^{+} $CD4^{+}$ T cells, confirming both the proliferative capacity and specificity of the TET_{751}^{+} cells (Supp Fig 1B).

S_{751}-specific T cells are not cross-reactive with human coronaviruses

SARS-CoV-2 spike cross-reactive CD4 T cells have been identified in uninfected individuals and linked to sequence conservation between SARS-CoV-2 and endemic human coronaviruses (hCoV), particularly within the S2 domain of spike[27,28]. Alignment of the spike protein sequences for SARS-CoV-2 and hCoV (NL63, 229E, OC43 and HKU1) demonstrated a low degree of conservation among residues within the S_{751} epitope (Supp Fig 1C). Prediction of epitope recognition by NetMHCII 2.3 suggested that an epitope present in NL63 and 229E (Supp Fig 1C) could potentially bind HLA-DRB1*15:01 with a similar affinity to the S_{751} epitope. To assess the extent of cross-recognition of these epitopes, we stimulated PBMC *in vitro* for 11 days with either the SARS-CoV-2-derived S_{751} peptide or analogous hCoV-derived peptides from NL63, OC43 or 229E, in the presence of IL-2. Staining with the S_{751} tetramer demonstrated robust recognition of cells expanded by the SARS-CoV-2 S_{751} peptide, but minimal expansion of cross-reactive cells by hCoV-derived peptides (Supp Fig 1D). To confirm this result, we independently stimulated PBMC with the S_{751} peptide for 11 days and then re-stimulated the cultures with either S_{751} or corresponding hCoV peptides. Expanded cultures showed strong AIM and CD154 responses to S_{751}, but failed to respond to the analagous hCoV peptides (Supp Fig 1E). Together, these data indicate that S_{751}-specific T cells do not exhibit cross-reactivity with hCoV spike proteins, and that cells identified by the DRB1*15:01/S_{751} tetramer represent a primary response to SARS-CoV-2 spike.

S_{751}-specific CD4 T cell memory is established following mild/moderate COVID-19 infection

We next studied TET_{751}^+ T cells in a well-characterised cohort[3,22] of individuals recovered from mild/moderate COVID-19 with the HLA-DRB1*15 allele (Supplemental Table 2; gating in Supp Fig 2). Among convalescent individuals with samples collected 20-60 days post-symptom onset (n=19), the median frequency of TET_{751}^+ cells was 0.0136% (IQR: 0.0095-0.0224%; Fig 2A), approximately 34-fold higher than in HLA-DRB1*15 uninfected, unvaccinated subjects. Antigen-experienced TET_{751}^+ cells were predominately $CCR7^+CD27^+$ (median 82.6%, IQR:70.9-88.4%), and were enriched for this T_{CM} phenotype relative to the bulk $CD4^+$ T_{mem} population (p=0.0004; Fig 2B).

Longitudinal analysis of bulk S-specific $CD4^+$ T cell responses by AIM assay has previously estimated a half-life ($T_{1/2}$) of 94 – 207 days over the first 4 to 8 months post-infection[14,22,29]. To refine the kinetics of the CD4 T cell response at the level of a single epitope, we longitudinally tracked the frequency of TET_{751}^+ cells in 21 individuals over a timecourse bridging 23 to 450 days post-symptom onset (Fig 2C). Notably, direct staining with the DRB1*15:01/S_{751} tetramer allowed for the identification of epitope-specific T cells even at timepoints when S_{751} peptide-specific responses were undetectable by AIM assay (Supp Fig 3A). TET_{751}^+ T cells declined rapidly during early convalescence, with an estimated half-life ($T_{1/2}$) of approximately 20 days (95% CI: 13-30 days; Fig 2C, Supp Fig 3B), before reaching a level of stable maintenance with a longer $T_{1/2}$ of ~377 days (95% CI: 283-503 days; Fig 2C, Supp Fig 3B). Notably, the median frequency of TET_{751}^+ cells at days 365 – 450 (n=17) was 0.0038% (IQR: 0.0024-0.0061), approximately 3.6-fold lower than during early convalescence but still significantly higher than uninfected controls (Supp Fig 3C).

Spike-specific $CD4^+$ T cell responses identified by AIM assays exhibit diverse T helper phenotypes, with prominent $CCR6^+CXCR3^-$ and $CCR6^-CXCR3^+$ antigen-specific memory

populations[3,5]. While *ex vivo* activation phenotypes cannot be assessed by AIM or ICS, TET_{751}^+ T cells showed evidence of activation (measured by CD38 expression) for >60 days before returning to a resting phenotype (Fig 2D). During early convalescence, TET_{751}^+ cells exhibited either a $CCR6^-CXCR3^+$ (median 46.0%, IQR: 36.1-53.9%) or $CCR6^-CXCR3^-$ phenotype (median 38.20%, IQR: 33.8-50.4%; Fig 2E). In contrast to the prominent $CCR6^+$ S-specific population previously identified by AIM[3,5], TET_{751}^+ cells were rarely $CCR6^+$. Over time, TET_{751}^+ cells tended to become proportionally enriched for CXCR3 expression, with a significant increase in the frequency of $CCR6^-CXCR3^+$ cells among the TET_{751}^+ population in samples collected more than 120 days post-symptom compared to samples collected during early convalescence (p=0.0003, Fig 2E, F).

S_{751}-specific $CD4^+$ T cell memory includes cells with a cTFH phenotype

Similar to other viral infections, the frequency and phenotype of spike-specific cTFH correlate with neutralising antibody titres following COVID-19[3,4,6,30]. During early convalescence (20-60 days post-symptom onset), a median of 9.9% (IQR: 5.6-18.4%) of TET_{751}^+ cells were cTFH ($CD4^+CXCR5^+$; Fig 3A), broadly similar to the median frequency of total $CD4^+$ T cells with a cTFH phenotype (11.2%, IQR: 6.1-13.7%; Fig 3A). The frequency of TET_{751}^+ cTFH declined over time in a single-phase pattern of decay with a $T_{1/2}$ of 227 days (95% CI: 179-287 days; Fig 2B, Supp Fig 3D). Among samples collected 365-450 days post-symptom onset, TET_{751}^+ cTFH were detectable (frequency ≥0.003%) in 13/17 (76.5%) individuals. In contrast to the phenotype of the bulk TET_{751}^+ population at early convalescence (Fig 2D), TET_{751}^+ cTFH predominately exhibited a $CCR6^-CXCR3^+$ phenotype (median 66.7%, IQR: 53.6-75.0%; Fig 3C). Overall, we find that even mild SARS-CoV-2 infection establishes long-lived spike-specific $CD4^+$ T cell memory with both cTFH and $CXCR5^-$ phenotypes.

Dynamics of S_{751}-specific CD4 T cells following SARS-CoV-2 vaccination

To assess S_{751}-specific T cell responses in the context of vaccination, we recruited 9 seronegative HLA-DRB1*15:01/02 participants without prior COVID-19 who were immunised with a COVID-19 vaccine (n=7 BNT162b2, n=1 ChAdOx nCoV-19, n=1 NVX-CoV2373; Supplementary Table 3). All vaccinees exhibited expansion of TET_{751}^+ T cells after a single dose, regardless of vaccine platform, with 8/9 exhibiting a further increase following dose 2 (Fig 4A).

Longitudinal sampling of BNT162b2-vaccinated individuals demonstrated a rapid expansion of TET_{751}^+ T cells as early as 7 days post-dose 1 (Fig 4B), with an increase in TET_{751}^+ cell frequencies over the next 21 days in all subjects (Fig 4B, C). Anti-S IgG titres were not detected above baseline until at least day 11 post-dose 1 (Supp Fig 4A), consistent with other reports that the induction of $CD4^+$ T cell responses precedes the serological response[18,28]. TET_{751}^+ T cell frequencies peaked 7-14 days after the second vaccine dose and were maintained above baseline throughout follow-up to 130 days (Fig 4C). The memory phenotype of TET_{751}^+ cells shifted from predominately T_{CM} ($CCR7^+CD27^+$; median 82.2%, IQR: 75.6-84.5%) after dose 1 to more heterogeneous $T_{CM}/T_{TM}/T_{EM}$ phenotypes after dose 2 (median 57.0% T_{CM}, IQR: 37.8-69.6%; Supp Fig 4B). T helper phenotype was relatively stable across doses, with the majority of TET_{751}^+ cells lacking either CCR6 or CXCR3 expression (Fig 4D).

Vaccine-induced activation of cTFH cells has proven to be an important correlate of the antibody response to immunisation[31-33], with antigen-specific cTFH serving as a better predictor of the magnitude of the serological response than $CXCR5^-$ T_{mem}[34]. The

218 $CD38^{+}ICOS+PD\text{-}1^{+}CXCR3^{+}$ cTFH population that emerges following influenza and yellow
219 fever vaccination contains a high proportion of vaccine-specific cTFH, and temporally
220 associates with the emergence of antibody secreting cells [31,35]. We therefore assessed both
221 total cTFH activation and TET_{751}^{+} cTFH frequencies following BNT162b2 vaccination.
222 There was limited evidence of a coordinated emergence of an activated cTFH population
223 following dose 1, with one subject showing an increase in $ICOS^{+}CD38^{+}$ cTFH at week 1
224 post-immunisation, and a second subject exhibiting a transient peak at week 3 (Supp Fig 4C).
225 Across all 7 participants, there was no further evidence for cTFH activation after dose 2
226 (Supp Fig 4C). Assessment of TET_{751}^{+} cTFH confirmed that, consistent with other
227 reports[10,18], vaccine dose 1 did drive expansion of antigen-specific cTFH in all particpants
228 (Fig 4E). Frequencies of TET_{751}^{+} cTFH remained relatively stable after vaccine dose 2, with
229 limited evidence of boosting in contrast to the total TET_{751}^{+} $CD4^{+}$ population (Fig 4E).
230 Nonetheless, TET_{751}^{+} cTFH exhibited a shift from a $CCR6^{-}CXCR3^{-}$ dominant phenotype
231 after dose 1 toward a $CCR6^{-}CXCR3^{+}$ phenotype following dose 2 (Supp Fig 4D). Overall, we
232 find that while primary immunisation elicits a spike-specific cTFH response, there is minimal
233 evidence for further cTFH activation or expansion following dose 2.
234
235 *The TCRαβ repertoire of vaccine-associated TET_{751}^{+} T cells is highly restricted*
236 Analysis of T cell receptor (TCR) repertoires has generated insight into the T cell response to
237 SARS-CoV-2, including the identification of CDR3 sequence motifs associated with disease
238 severity[36], and identification of cross-reactive TCR clonotypes present in uninfected
239 subjects[37,38]. We therefore single-cell sorted TET_{751}^{+} T cells from three uninfected vaccinees
240 and analysed *TRAV/TRBV* gene usage and CDR3 sequences. Among the 136 TCRαβ pairs
241 recovered, *TRBV* expression was highly skewed toward *TRBV24.1* (55% of recovered
242 sequences), *TRVB20.1* (18%) and *TRBV6.1* (9%) genes (Fig 4F). Comparison of *TRBV*

CDR3 sequences from these three families identified at least 5 public clonotypes shared between at least two of the three vaccinees (Supp Fig 5), with highly conserved *TRBV* CDR3 sequence motifs evident in both public and private clonotypes (Supp Fig 5). While there is little comparative data reported for other epitope-specific $CD4^+$ T cell responses, the TCR repertoire associated with HLA-DRB1*15/S_{751}-specific T cells appears tightly restricted, with more limited clonal diversity compared to repertoires described for some immunoprominent $CD8^+$ T cell populations[39].

Vaccination of individuals with previous COVID-19 rapidly recalls S_{751}-specific T cell memory

Numerous studies have established that single dose immunisation of COVID-19 convalescent individuals produces spike-specific antibody and T cell responses that match or exceed the response to two doses in immunologically naïve populations[17,40,41]. Serological responses are reported to peak by day 7 post-vaccination in convalescent subjects[42], but little is known about the recall kinetics of $CD4^+$ T cells within the first week after immunisation. We obtained longitudinal samples from 12 HLA-DRB1*15 individuals from the convalescent cohort who received at least one dose of a COVID-19 vaccine (n=7 ChAdOx nCoV-19, n=5 BNT162b2; Supplemental Table 2). Pre-vaccine baseline samples were collected no more than 4 months prior to immunisation, and participants were vaccinated a median of 441 days post-SARS-CoV-2 symptom onset. Consistent with other cohorts, neutralising antibody titres among the convalescent cohort two weeks after a single immunisation were significantly higher than titres among the uninfected cohort after either dose (Fig 5A).

Robust expansion of TET_{751}^+ T cells was observed 1-2 weeks after primary immunisation (Fig 5B). Vaccination with the adenoviral vaccine resulted in a median 6.4-fold increase of

TET_{751}^+ cells (IQR: 3.4-8.7), while mRNA vaccination drove significantly greater expansion (median 17-fold, IQR: 13.6-26.3; Fig 5C). To precisely map the kinetics of antigen-specific T cell recall, we analysed samples from day 3 to day 65 post-vaccination. At day 3, the frequency of TET_{751}^+ cells in the circulation consistently declined relative to baseline samples (Fig 5D, E), likely reflecting activation and/or retention of antigen-specific cells in lymphoid tissues. By day 5, robust CD4 T cell proliferation was evident, with the frequency of TET_{751}^+ cells peaking between days 5 and 12 post-vaccination (Fig 5D, E). While contraction of the S_{751}-specific response could not be followed in BNT162b2-vaccinated subjects due to the 3 week boost schedule, subjects vaccinated with ChAdOx nCoV-19 exhibited a gradual decline in TET_{751}^+ cells over the course of 40 days after their first dose (Fig 5D). In contrast to the predominant resting T_{CM} phenotype of S_{751}-specific T cells generated after infection, early recall responses (days 5-10 post-vaccination) exhibited a notable shift toward T_{TM} ($CCR7^-CD27^+$) and T_{EM} ($CCR7^-CD27^-$) phenotypes (Fig 5E). By day 12, however, TET_{751}^+ cells largely returned to a T_{CM}-dominated phenotype (Fig 5E). The shift in memory status of antigen-specific cells coincided with transiently high levels of $CXCR3^+$ expression (Fig 5E), potentially reflecting recall of the CXCR3-biased population of resting memory TET_{751}^+ T cells observed during late convalescence.

S_{751}-specific cTFH are transiently activated by vaccination in convalescent subjects

In contrast to the variable and uncoordinated changes in $ICOS^+CD38^+PD\text{-}1^+$ cTFH after single-dose vaccination of the naïve cohort, activated cTFH were rapidly and transiently induced by vaccination of convalescent subjects (Fig 6A; Supp Fig 6A). The appearance of activated cTFH occurred as early as day 4 post-vaccination and typically waned by day 12 (Fig 6A). Compared to parental cTFH, these activated cells were enriched for CXCR3 expression (Fig 6B), resembling the cTFH1 cells that are recalled by annual influenza

vaccination. Previous work has suggested that ~40% of activated cTFH exhibit specificity for vaccine antigens[31], but pMHC tetramers offer the opportunity to determine the prominence of individual epitopes in this population. Across individuals, the frequency of S_{751}-specific cells within $ICOS^+CD38^+$ cTFH ranged from less than 1% up to 11.9% (Fig 6C).

While these data and other studies clearly suggest that activated cTFH contain a high frequency of vaccine antigen-specific cells, the persistence and long-term activation state of these cells is less clearly defined. By tracking both the frequency and phenotype of TET_{751}^+ cTFH, we find these cells are recalled by vaccination with similar kinetics to $CXCR5^-$ cells, and persist in the circulation for substantially longer than the $ICOS^+CD38^+$ cTFH population (Fig 6D). Phenotypic analysis of TET_{751}^+ cTFH clearly demonstrated that while this population emerges at day 5 post-vaccination with an $ICOS^+CD38^+PD\text{-}1^+$ phenotype (Supp Fig 6B), ICOS and CD38 are rapidly lost from TET_{751}^+ cells over the subsequent 7 days (Fig 6E, F). By four weeks post-vaccination, less than 50% of S_{751}-specific cTFH expressed PD-1 (Fig 6G), indicating that recalled antigen-specific cTFH can persist in the circulation as a resting, $CD38^-ICOS^-PD\text{-}1^{+/-}$ pool. Together, these data indicate that while recalled antigen-specific cTFH emerge in the circulation as an activated population, enumeration of activated or $PD\text{-}1^+$ cTFH likely underestimates the total spike-specific population over time.

S_{751}-specific clonotypes established by infection are recalled by vaccination and exhibit both cTFH and $CXCR5^-$ phenotypes

To more precisely track the recall of S_{751}-specific T cell memory, and to investigate the clonal relationship between $CXCR5^-$ T_{mem} and cTFH populations, we sequenced 187 TET_{751}^+ cells collected at early convalescence, day 8 post-vaccination and day 29 post-vaccination in a convalescent individual (CP24). Following infection, 27 clonotypes represented ~80% of

318 the sequenced TCR repertoire (Fig 7A). 9 of these clonotypes were identified in the
319 subsequent samples, comprising ~20% of the post-vaccine repertoire and directly
320 demonstrating recruitment of S_{751}-specific infection-induced memory into the recall response
321 (Fig 7A). Across all timepoints, *TRAV* and *TRBV* gene usage was biased similarly to that of
322 the naïve vaccine cohort, with TET_{751}^{+} cells exhibiting prevalent TRBV20.1, 24.1 and 6.1
323 usage (Fig 7B). Indeed, multiple clonotypes identified from one donor, CP24, were shared
324 with naïve vaccinees (Table/Fig), suggesting that T cells recognise spike-derived epitopes
325 similarly across infection and primary vaccination. Finally, we compared the clonotypic
326 composition of TET_{751}^{+} cTFH and CXCR5- T_{mem} populations to understand the degree of
327 clonal overlap between these functionally distinct $CD4^{+}$ T cell subsets. Across the three
328 timepoints, all 21 cTFH-derived clonotypes were also identified among TET_{751}^{+} $CXCR5^{-}$
329 cells (Fig 7C), indicating that spike-specific T cell clonotypes can be recruited into both the
330 T_{mem} and cTFH compartments.

Discussion:

Traditional intracellular cytokine stimulation (ICS) and, more recently, AIM assays have been instrumental in defining the $CD4^+$ T cell response to SARS-CoV-2 antigens. However, the identification of immunogenic peptides and the use of HLA class II tetramers to define epitope-specific T cells now allows for a detailed characterisation of the *ex vivo* phenotype and precise dynamics of memory T cell and cTFH populations. We find that S_{751}-specific T cells were detected in both convalescent and vaccinated subjects at frequencies comparable to other reported HLA class I[39,43,44] and II[18,45]-restricted SARS-CoV-2 epitope-specific responses. Although there are a lack of studies assessing epitope-specific CD4 responses during COVID-19 convalescence, the median S_{751}-specific T cell frequencies detected over one year of follow-up (138 TET_{751}^+ cells/10^6 $CD4^+$ cells during early convalescence to 41 TET_{751}^+ cells/10^6 $CD4^+$ cells at >1 year) are similar to frequencies of epitope-specific T cells following influenza infection[46], RSV infection[47], or vaccination with the live attenuated yellow fever virus vaccine[48]. Interestingly, while SARS-CoV-2 HLA class I-restricted $CD8^+$ T cell responses have been reported to be stable over the course of convalescence[39,43], we observe a rapid decline in TET_{751}^+ cells during the first four months after symptom onset, followed by stable memory frequencies within both $CXCR5^-$ and cTFH populations beyond one year post-symptom onset.

Perhaps the most pertinent difference between the spike-specific $CD4^+$ T cell responses detected by the S_{751} tetramer and previous studies using the AIM assay lies in the frequency of $CCR6^+$ antigen-specific cells. Both we[3,22] and others[5,14] find a substantial proportion of S-specific AIM^+ $CD4^+$ T cells express CCR6, albeit in the absence of IL-17 production[3]. While similar phenotypes were observed for S_{751}-specific cells identified by AIM (via OX-40 and CD25/CD137)[22], the HLA-DRB1*15:01/S_{751} tetramer identified only a negligible frequency

of $CCR6^+$ cells. Whether these cells exhibit lower affinity for pMHCII and are therefore poorly stained by the HLA-DRB1*15:01 tetramer or represent cells upregulating CCR6 upon stimulation is currently unclear, but should be investigated in future studies.

In contrast to serological responses[40,49], less is known about the early induction of $CD4^+$ T cell responses by SARS-CoV-2 vaccines, in either previously uninfected or convalescent subjects. We find clear evidence of S_{751}-specific CD4 T cell responses to the mRNA BNT162b2 vaccine by day 7 post-vaccination in naïve individuals, consistent with AIM data[28] and recent longitudinal tracking of another HLA-DRB1*15:01-restricted spike-derived epitope[18]. Our data indicate that infection and primary vaccination elicit similar frequencies of TET_{751}^+ T cells, albeit with differences in CXCR3 expression that may reflect distinct cytokine microenvironments during T cell priming. After two vaccine doses, S_{751}-specific T cell frequencies among the naïve cohort were comparable to single-dose vaccinated convalescent subjects, in contrast to the elevated neutralising antibody titres among the convalescent cohort.

Robust cTFH recall was a prominent feature of vaccination of convalescent subjects. Whether such responses are a feature of 'hybrid immunity'[16] (infection followed by vaccination) or the long duration (~1 year) between the immunological 'prime' and vaccine boost is currently difficult to define. Nonetheless, identification of S_{751}-specific cTFH provided a unique opportunity to study aspects of cTFH memory and recall that are typically challenging to study in human cohorts. Herati *et al* provided some of the first evidence that that resting $CXCR5^+CD38^-ICOS^-$ cells may serve as a reservoir of influenza-specific cTFH memory that is recalled by subsequent vaccination[32]. Our results further advance this concept, as we find that mild/moderate SARS-CoV-2 infection induces long-lived spike-

specific cTFH memory in the majority of participants. A high degree of clonal overlap between S_{751}-specific CXCR5$^-$ T_{mem} and cTFH suggests a lack of preferential recruitment for specific T cell clones into the TFH pool. However, the relative contributions of T_{mem} and cTFH into the recall response are difficult to determine from the current data, and will require analysis of additional epitopes or TCR sequences. After vaccination, we show that S_{751}-specific cTFH re-acquire a resting phenotype (CD38$^-$ICOS$^-$) within 2 weeks, and later substantially downregulate PD-1 expression. Therefore, while the study of CD38$^+$ICOS$^+$, or even PD-1$^+$, cTFH captures antigen-specific cells during acute timepoints after vaccination or infection, the accurate enumeration and phenotypic characterisation of memory cTFH likely requires antigenic re-stimulation or pMHC complexes.

Overall, we find COVID-19 generates a stable pool of spike-specific cTFH and memory CD4$^+$ T cells that are recalled upon antigen re-exposure. The establishment of similar frequencies of long-lived T cell memory by both infection and vaccination suggests that even in the context of waning vaccine efficacy, SARS-CoV-2 booster vaccines should efficiently recall spike-specific CD4$^+$ T cell responses. The capacity of spike-based vaccines to elicit a robust cTFH1 recall response, which is positively associated with neutralizing antibody titres in multiple studies[3-6], highlights the utility of these cells in tracking vaccine immunogenicity. Future studies linking lymphoid GC and circulating TFH using MHC class II tetramers will provide further understanding of the relationship between CXCR3$^+$ cTFH and GC TFH.

<u>Limitations:</u> Studies of epitope-specific T cell responses often face cohort size limitations, due to the need to recruit individuals with specific HLA alleles. Additionally, we acknowledge that the dynamics of S_{751}-specific T cells may not be representative of all spike-specific (or even SARS-CoV-2-specific) T cells. This is particularly relevant to epitopes with

406 cross-reactivity between SARS-CoV-2 and other antigens. It should be noted the uninfected
407 vaccine cohort was younger than the COVID-19 convalescent cohort (median 44 vs 58
408 years), although multiple studies have suggested that there is no correlation between age and
409 $CD4^+$ T cell SARS-CoV-2 vaccine responses[40,50]. Future studies will benefit from larger
410 cohorts that include individuals with more severe COVID-19, as well as tracking of multiple
411 immunogenic epitopes to compare CD4 T cell responses across both spike and non-spike
412 proteins.
413

Methods:

Participant recruitment and sample collection

The study protocols were approved by the University of Melbourne Human Research Ethics Committee (#2056689 and #21198153983), and all associated procedures were carried out in accordance with the approved guidelines. All participants provided written informed consent in accordance with the Declaration of Helsinki.

A longitudinal cohort of subjects recovered from COVID-19 (previously described in Juno *et al*[3] and Wheatley *et al*[22]) were recruited to provide additional blood samples following vaccination against SARS-CoV-2. All cohort participants had either a prior +ve nasal PCR during early infection for SARS-CoV-2 or clear exposure to SARS-CoV-2 as well as a positive ELISA for SARS-CoV-2 S and RBD protein as previously reported[3]. Contemporaneous controls who did not experience any symptoms of COVID-19 and who were confirmed to be seronegative were also recruited to provide blood samples prior to and following vaccination for SARS-CoV-2. For all participants, whole blood was collected with sodium heparin anticoagulant. Plasma was collected and stored at -80ºC, and PBMCs were isolated via Ficoll-Paque separation, cryopreserved in 90% fetal calf serum (FCS)/10% DMSO and stored in liquid nitrogen. All participants were HLA typed by the Victorian Transplantation and Immunogenetics Service.

Generation of MHC II tetramers

Human DRB1*15:01 NLLLQYGSFCTQLNRAL (SARS-CoV-2) and DRA1*01:01/DRB1*15:01 PVSKMRMATPLLMQA (CLIP) biotinylated monomers were generated by ProImmune. Biotinylated monomers were tetramerised by sequential addition of streptavidin-PE (BD Biosciences) or -APC (BioLegend).

Tetramer staining

Cryopreserved PBMC samples were thawed in RPMI-1640 with 10% fetal calf serum and pen/strep (RF10), washed, and counted. Up to 10 x 10^6 PBMC were washed in 2% FCS/PBS prior to incubation in 50nM Dasatinib (Sigma) for 30 min at 37ºC. APC- or PE- conjugated tetramer was then added at 4µg/mL for 60 min at 37ºC. Cells were washed in PBS, stained with Live/Dead fixable green dead cell stain (Life Technologies), and incubated for 30 min at 4ºC with a surface stain antibody cocktail. Surface stain antibodies included: CD45RA PerCP-Cy5.5 (HI100), CCR7 Alexa Fluor 647 (G043H7), CD69 APC Fire-750 (FN50), CD27 BV510 (MT-T271), CD4 BV605 (RPA-T4), PD-1 BV650 (EH12.2H7), CCR6 BV785 (G034E3) and CXCR3 PE Dazzle594 (G02H57) (BioLegend), CD38 Alexa Fluor 700 (HIT2), ICOS BV421 (C398.4), CD3 BUV395 (SK7) and CD20 BUV805 (2H7) (BD Biosciences), and CXCR5 PE-Cy7 (MU5UBEE; Thermo Fisher). Cells were then washed with 2% FCS/PBS and fixed with cytofix (BD Biosciences), prior to acquisition on a LSR Fortessa (BD Biosciences). Data was analysed using Flowjo v10.2 (TreeStar).

Activation induced marker (AIM) assay

Cyropreserved PBMC samples were thawed, seeded at 1 – 2 x 10^6 cells/well of a 96-well plate, and rested for 4 hr at 37ºC. Cells were then stimulated with 1µg/mL of peptide or an equivalent volume of DMSO for 20 hr. In some experiments, CD154 APC-Cy7 (TRAP-1, BD Biosciences) antibody was included in the culture medium for the duration of the stimulation. Cells were then washed in PBS and stained with Live/Dead green, and surface stained with the following antibodies: OX-40 PerCP Cy5.5 (Ber-ACT35), CD25 APC (BC96) BL, CD137 BV421 (4-B41), CD27 BV510 (MT-T271), CD4 BV605 (RPA-T4), CCR6 BV785 (G034E3) and CXCR3 PE Dazzle594 (G02H57) (BioLegend), CD45RA PE-Cy7 (HI100) and CD3 BUV395 (SK7) (BD Biosciences), and CXCR5 PE (MU5UBEE,

Thermo Fisher). For HLA blocking experiments, PBMCs were pre-incubated with 8μg/mL of purified HLA-DR (L243, BioLegend), or mouse IgG k isotype control (MOPC-21, BioLegend) for 1 hr prior to peptide stimulation.

In vitro S_{751} proliferation assay

To expand S_{751}-specific T cells in vitro, 3 – 5 x 10^6 freshly isolated or thawed cryopreserved PBMC samples were seeded in 96-well plates and stimulated with 1μg/mL of SARS-CoV-2 S_{751}, NL63 S_{801}, 229E S_{618}, OC43 S_{833} or an equivalent volume of DMSO for 9 – 10 days. At days 3/4 and 6/7, the culture medium was replenished and supplemented with 10U/mL recombinant human IL-2 (Peprotech). On day 9 or 10, cells were stained for S_{751} tetramer or antigen specific responses measured via AIM assay. In some experiments, cells were stained with 2.5μM Cell trace violet proliferation dye (Thermo Fisher) prior to stimulation with peptide S_{751}. In such cases, PBMCs were cultured for 6 days and supplemented with 10U/mL IL-2 at day 3.

Single cell sorting and TCR sequencing

Up to 10 x 10^6 thawed PBMC were stained with tetramer, followed by viability staining with Live/Dead green. Cells were then surface stained for 30 min at 4°C with: CD45RA PerCP-Cy5.5 (HI100), CCR7 Alexa Fluor 647 (G043H7), CD4 BV605 (RPA-T4), CCR6 BV785 (G034E3) and CXCR3 PE Dazzle594 (G02H57) (BioLegend), CD3 APC-H7 (SK7) and CD20 BV510 (2H7) (BD Biosciences), and CXCR5 PE-Cy7 (MU5UBEE, Thermo Fisher). Cells were sorted into 96-well plates using a BD FACS Aria III sorter and frozen until cDNA synthesis. cDNA was synthesized by reverse transcription using 450ng random hexamer primers, 2ul of 10mM dNTP, 0.1M DTT, 0.25% v/v Igepal, RNAsin® (Promega) and 120U Superscript III reverse transcriptase (Invitrogen). PCR was performed at 42 °C for 10 min,

25 °C for 10 min, 50 °C for 60 min and 94 °C for 5 min, and cDNA stored at − 20 °C. *TRAV* and *TRBV* genes were amplified by nested PCR. First round PCR reactions were prepared using 10ul of cDNA template, 10mM dNTP, HotStar Taq Plus Polymerase and the following primers as described in Dash *et al*[51]: TRAC-EXT, TRAV-EXT (cocktail), TRBC-EXT, TRBV-EXT (cocktail). Secondary PCR reactions were carried out independently for *TRAV* or *TRBV* transcripts using 2.5ul of unpurified primary PCR product and either TRAC-INT/TRAV-INT primers or TRBC-INT/TRBV-INT primer cocktails. All nested PCR reactions were performed for 40 cycles at 95 °C for 20 s, 52 °C for 30 s, and 72 °C for 45 s. Recovered PCR products were subject to Sanger sequencing and productive T cell receptor sequences were aligned using IMGT[52]. Analysis of clonotype sharing between subjects or timepoints was performed using the Immunarch package (Immunomind) in R 3.6.2. Visualisation of alpha and beta V gene pairing was performed using Circlize[53].

ELISA

96-well Maxisorp plates (Thermo Fisher) were coated overnight at 4° C with 2_ µg/mL recombinant SARS-CoV-2 S proteins (Hexapro). After blocking for 1 hour, room temperature with PBS + 1% FCS, plasma samples were serially diluted in PBS + 1% FCS prior to incubation for two hours at room temperature. Plates were then washed using PBST prior to incubation with 1:20000 dilution of HRP-conjugated anti-human IgG (Sigma) for 1 hour. Plates were washed and developed using TMB substrate (Sigma), stopped using 0.16 M sulphuric acid and read at 450 nm. Endpoint dilutions were calculated using a fitted curve (4 parameter log regression) and Prism 9.0 software (Graphpad).

Microneutralisation assay with ELISA-based read out

Wildtype SARS-CoV-2 (CoV/Australia/VIC/01/2020) isolate was passaged in Vero cells and stored at -80ºC. 96-well flat bottom plates were seeded with Vero cells (20,000 cells per well in 100µl). The next day, Vero cells were washed once with 200 µl serum-free DMEM and added with 150µl of infection media (serum-free DMEM with 1.33 µg/ml TPCK trypsin). 2.5-fold serial dilutions of heat-inactivated plasma (1:20-1:12207) were incubated with SARS-CoV-2 virus at 2000 $TCID_{50}$/ml at 37ºC for 1 hour. Next, plasma-virus mixtures (50µl) were added to Vero cells in duplicate and incubated at 37ºC for 48 hours. 'Cells only' and 'virus+cells' controls were included to represent 0% and 100% infectivity respectively. After 48 hours, all cell culture media were carefully removed from wells and 200 µl of 4% formaldehyde was added to fix the cells for 30 mins at room temperature. The plates were then dunked in a 1% formaldehyde bath for 30 minutes to inactivate any residual virus prior to removal from the BSL3 facility. Cells were washed once in PBS and then permeabilised with 150µl of 0.1% Triton-X for 15 minutes. Following one wash in PBS, wells were blocked with 200µl of blocking solution (4% BSA with 0.1% Tween-20) for 1 hour. After three washes in PBST (PBS with 0.05% Tween-20), wells were added with 100µl of rabbit polyclonal anti-SARS-CoV N antibody (Rockland, #200-401-A50) at a 1:8000 dilution in dilution buffer (PBS with 0.2% Tween-20, 0.1% BSA and 0.5% NP-40) for 1 hour. Plates were then washed six times in PBST and added with 100µl of goat anti-rabbit IgG (Abcam, #ab6721) at a 1:8000 dilution for 1 hour. After six washes in PBST, plates w ere developed with TMB and stopped with 0.15M H_2SO_4. OD values read at 450nm were then used to calculate %neutralisation with the following formula: ('Virus + cells' – 'sample') ÷ ('Virus + cells' – 'Cells only') × 100. IC_{50} values were determined using four-parameter nonlinear regression in GraphPad Prism with curve fits constrained to have a minimum of 0% and maximum of 100% neutralisation.

Statistics

To compare the decay phase of CD4 and Tfh cells after the peak, we modeled a fraction *f* of cells at the peak as short-lived cells, and the remainder (1−*f*) as long-lived cells, which decay independently. The model can be written as:

$$Y(t) = Y_0\left[fe^{-\delta_1 t} + (1-f)e^{-\delta_2 t}\right]$$

in which:

Y_0 = peak levels of cells

f = fraction of short-lived cells

δ_1 = death rate of short-lived cells

δ_2 = death rate of long-lived cells.

Censored non-linear mixed effect model was used to fit the model to the longitudinal T cell data. The limit of detection was fixed to 0.0001% (for total CD4) and 0.003% (for Tfh population). We also tested if the data can be fitted with just a single decay (ie, setting $f = 1$ and $\delta_2 = 0$ in the equation above) or using the non-constrained equation (a bi-phasic model with both f and δ_2 as free parameters). Model comparison was performed based on the likelihood ratio test by comparing the likelihood value of the nested models and the difference in the number of parameters. These analyses were carried out in Monolix R2019B.

Flow cytometry data was analysed with FlowJo v10.2. Statistical analysis was performed in GraphPad Prism 9 (TreeStar) using non-parametric statistical tests as indicated. $P<0.05$ was considered significant.

Data Availability: All data are available from the corresponding authors upon reasonable request.

Acknowledgements: The authors would like to thank the study participants for their involvement and provision of samples. We thank Vanta Jameson at the Melbourne Cytometry Platform (Melbourne Brain Centre node) for the provision of cell sorting services, and Caroline Batten for technical assistance.

Funding: This work was funded by a NHMRC Ideas Grant to JAJ (GNT2004398), NHMRC program grant to SJK and MPD (1149990), an MRFF grant to JAJ, AKW and SJK (GNT2005544) and the Victorian Government. MK, MPD, AKW and SJK are funded by NHMRC Investigator grants.

Conflicts: The authors declare no conflicts of interest.

Figure Legends:

Figure 1. Specificity of HLA-DRB1*15:01/S_{751} tetramers. (A) Staining of HLA-DRB1*15:01/S_{751} tetramer on cryopreserved PBMC from individuals recovered from mild COVID-19 infection with or without the HLA-DRB1*15 allele. (B) Tetramer staining on PBMC collected prior to or after 2 doses of BNT162b2 vaccine in individuals with or without the HLA-DRB1*15 allele. (C) Co-staining of PBMC from a BNT162b2 vaccinated individual with HLA-DRB1*15:01 tetramers loaded with S_{751} or an irrelevant control peptide. (D) Co-staining of CD45RA and S_{751} tetramer following BNT162b2 vaccination.

Figure 2. Establishment of S_{751}-specific $CD4^+$ T cell memory following mild COVID-19. (A) Frequency of TET_{751}^+ cells (as % of total $CD4^+$) among uninfected (n=9) or COVID-19 convalescent individuals sampled 20 to 60 days post-symptom onset (n=19). (B) Representative plots demonstrating expression of CCR7 and CD27 on TET_{751}^+ or bulk T_{mem}

588 (non-naïve $CD4^+$) subsets. Comparison of T_{CM} ($CCR7^+CD27^+$) phenotype between tet^+ or
589 bulk T_{mem} assessed using Wilcoxon test (n=19). (C) Representative staining and frequencies
590 of TET_{751}^+ cells over the course of 1 to 15 months post-symptom onset (n=21). (D)
591 Expression of CD38 on TET_{751}^+ cells during longitudinal follow-up (n=19 at d20-60 and
592 d>120; n=15 at d61-120). Statistics assessed by Kruskal-Wallis and Dunn's multiple
593 comparisons test (**p<0.01, ****p<0.001). (E, F) Expression of CCR6 and CXCR3 on
594 TET_{751}^+ or T_{mem} cells during (E) early or (F) late convalescence (n=19). Lines indicate
595 median and IQR. Statistics assessed by Wilcoxon test.
596
597 **Figure 3. Frequency and phenotype of $CXCR5^+$ S_{751}-specific cTFH.**
598 (A) Representative staining and frequency of $CXCR5^+$ cells among $CD4^+$ T_{mem} and TET_{751}^+
599 cells at days 20-60 post-symptom onset (n=19). Statistics assessed by Wilcoxon test. (B)
600 Longitudinal analysis of the frequency of TET_{751}^+ cells among the cTFH ($CXCR5^+$ T_{mem})
601 population (n=21). (C) Expression of CCR6 and CXCR3 among TET_{751}^+ (blue) or bulk (grey)
602 cTFH at 20-60 days post-symptom onset (n=19). Graph indicates median and IQR.
603
604 **Figure 4. Induction of S_{751}-specific CD4 T cells following vaccination.**
605 (A) Frequencies of S_{751}-specific T cells at baseline, week 3 post-dose 1, or week 2 post-dose
606 2 among 9 previously uninfected individuals. Blue, BNT162b2; red, ChAdOx-nCoV19;
607 green, NVX-CoV2373. (B) Representative staining of S_{751} tetramer among $CD4^+$ T cells
608 following immunization with one dose of BTN12b2 in a previously uninfected subject. (C)
609 Longitudinal S_{751}-specific T cell frequencies at baseline and following BNT162b2
610 vaccination among 7 previously uninfected individuals. Closed circles, samples collected
611 after dose 1; open circles, samples collected after dose 2. (D) CCR6 and CXCR3 expression
612 on TET_{751}^+ cells at week 3 post-dose 1 or week 2 post-dose 2 among 7 individuals vaccinated

with BNT162b2. (E) Longitudinal S_{751}-specific cTFH frequencies at baseline and following BNT162b2 vaccination among 7 previously uninfected individuals. Closed circles, samples collected after dose 1; open circles, samples collected after dose 2. (F) Circos plots indicating pairing of TRAV and TRBV genes among sorted TET_{751}^+ cells for three subjects after the second vaccine dose.

Figure 5. Recall of S_{751}-specific $CD4^+$ T cells following vaccination of COVID-19 convalescent individuals. (A) Neutralising antibody titres against SARS-CoV-2 among the naïve vaccination cohort (3 weeks post-dose 1, or 3 weeks post-dose 2; n=9) and convalescent subjects (2 weeks post-dose 1, n=10). (B) Changes in TET_{751}^+ T cell frequency between pre-vaccine and post-vaccine (1-2 weeks post-dose 1) among convalescent subjects. (C) Fold change in TET_{751}^+ T cell frequencies according to vaccine platform. (D) Time course of S_{751}-specific T cell expansion in a single convalescent individual prior to and following a single dose of BNT162b2. (E) Longitudinal tetramer frequencies among 12 individuals (n=7 AstraZeneca, red; n=5 Pfizer/BioNTech, blue). Pre-vaccine samples are set at day -1. Blue shading indicates days 3-4 post-immunization, red indicates days 4-12. (F) Expression of CCR7/CD27 and CCR6/CXCR3 on TET_{751}^+ cells at early (days 5-10) or late (day >11) timepoints after vaccination. N=5 ChAdOx nCoV19, red; n=5 BNT162b2, blue; statistics assessed by Wilcoxon test.

Figure 6. Vaccine-associated recall of activated and S_{751}-specific cTFH. (A) Representative staining and frequency of $ICOS^+CD38^+$ cTFH following single dose vaccination of convalescent subjects (n=12). Grey shading indicates days 4-11 post-vaccination. (B) Representative staining of CCR6 and CXCR3 on total cTFH ($CD4^+CXCR5^+$) or $ICOS^+CD38^+$ cTFH. Data are representative of 10 individuals with

638 samples available from day 5-11 post-vaccination. (C) S_{751} tetramer binding within the
639 $ICOS^+CD38^+$ cTFH population in two subjects with low (<1%) or high (>10%) S_{751}-specific
640 frequencies. (D) Longitudinal S_{751}-specific cTFH frequencies among n=12 convalescent
641 subjects following vaccination. Limit of detection, 0.003% (indicated by dashed line). (E)
642 Expression of ICOS and CD38 on TET_{751}^+ cTFH (blue) in a single individual over time. (F)
643 Proportion of S_{751}-specific cTFH with an activated ($ICOS^+CD38^+$) phenotype over time
644 (n=10). (G) Expression of PD-1 on S_{751}-specific cTFH following vaccination (n=10).
645
646 **Figure 7. Longitudinal tracking of S_{751}-specific TCR clonotypes.** (A) Persistence of
647 TRBV clonotypes across three longitudinal samples in a single convalescent individual.
648 Colours identify the 27 most frequent clonotypes comprising 80% of the recovered repertoire
649 at the day 70 convalescent timepoint. (B) Circos plots indicating TRAV and TRBV pairing at
650 each indicated timepoint. (C) Clonotype sharing between cTFH and $CXCR5^-$ T_{mem} across
651 among cells recovered from any timepoint.
652

Supplemental Table 1. HLA alleles among participants tested for $CD4^+$ T cell AIM responses to S_{751} peptide.

Participant	S_{751} response	HLA-DRB1	HLA-DP	HLA-DQ
CP02	Yes	04:01, 15:01	DPB1*04:01 DPA1*01:03	DQB1*03:02/289, 06:02 DQA1*01:02, 03:03
CP24	Yes	01:01, 15:01	DPB1*04:01 DPA1*01:03	DQB1*05:01, 06:02 DQA1*01:01, 01:02
CP39	Yes	07:01, 15:01	DPB1*03:01, 04:01 DPA1*01:03	DQB1*02:02/156/163N, 06:02 DQA1*01:02, 02:01
CP60	Yes	03:01, 15:01	DPB1*04:01 DPA1*01:03	DQB1*02:01/163N, 06:02 DQA1*01:02, 05:01
CP63	Yes	03:01, 07:01	DPB1*04:02, 15:01 DPA1*01:03, 01:04	DQB1*02:01/163N, 02:02/156/163N DQA1*02:01, 05:01
CP04	No	01:01, 03:01	DPB1*04:01 DPA1*01:03	DQB1*02:01, 05:01 DQA1*01:01, 05:01
CP12	No	04:01, 07:01	DPB1*04:01, 05:01 DPA1*01:03, 02:06	DQB1*03:02/289, 03:03 DQA1*02:01, 03:01
CP18	No	01:01, 04:01	DPB1*04:01 DPA1*01:03	DQB1*03:02/289, 05:01 DQA1*01:01, 03:01
CP30	No	03:01, 04:01	DPB1*04:01 DPA1*01:03	DQB1*02:01/163N, 03:01/276N DQA1*03:03, 05:01
CP42	No	03:01, 04:05	DPB1*04:01, 05:01 DPA1*01:03, 02:02	DQB1*02:01/163N, 02:02/163N DQA1*03:03, 05:01

Supplemental Table 2. Details of HLA-DRB1*15:01 COVID-19 convalescent cohort.

	Convalescent Cohort (n=21)	**Vaccine Sub-Cohort (n=13)**
Age (Median, IQR)	58 (51, 61)	58 (50, 60)
Sex – Female (n, %)	10 (48%)	7 (54%)
Disease severity – Mild (n, %)	13 (62%)	8 (62%)
Vaccination, days post-symptom onset (Median, IQR)		441 (419, 464)

Supplemental Table 3. Demographic and immunisation details of HLA-DRB1*15:01/02 uninfected vaccine cohort.

Participant	Age	Sex	Vaccine	Boost Interval
COR012	29	F	BNT162b2	29
COR021	30	M	BNT162b2	23
COR022	57	F	BNT162b2	22
COR024	33	F	BNT162b2	23
COR039	57	F	BNT162b2	21
COR281	42	F	BNT162b2	25
COR291	49	M	BNT162b2	21
COR032	22	F	ChAdOx-nCoV19	85
COR003	44	M	NVX-CoV2373	22

Supplemental Table 4. Public TRBV clonotypes shared by convalescent and uninfected vaccinee participants.

		Subjects	**Common TRAV**
TRBV 20.1	CSARRGTEAFF	COR12, COR22, CP24	TRAV8-2, TRAV8-4
TRBV 24.1	CATSAPDRGNNQPQHF	COR03, CP24	TRAV12-1
	CATSDFRVGDNQPQHF	COR12, CP24	TRAV12-1
	CATSDPDRGDNQPQHF	COR03, CP24	TRAV12-1
	CATSDPGQGDHQPQHF	COR03, CP24	TRAV12-1
	CATSDPGQGNNQPQHF	COR03, CP24	TRAV12-1, TRAV9-2
	CATSDPRQGDNQPQHF	COR03, COR22, CP24	TRAV12-1
	CATSDPRTGDNQPQHF	COR03, CP24	TRAV12-1
	CATSDPRVGDNQPQHF	COR03, COR12, CP24	TRAV12-1
	CATSDPSRGDNQPQHF	COR03, CP24	TRAV12-1
	CATSDVSGGNYNEQFF	COR03, CP24	TRAV13-2 TRAV1-2
TRBV 6-1	CASSEGASNQPQHF	COR03, COR12, COR22, CP24	TRAV12-1
	CASSEGVSNQPQHF	COR03, CP24	TRAV12-1

References:

1 Khoury, D. S. *et al.* Neutralizing antibody levels are highly predictive of immune protection from symptomatic SARS-CoV-2 infection. *Nature medicine* **27**, 1205-1211, doi:10.1038/s41591-021-01377-8 (2021).

2 Gilbert, P. B. *et al.* Immune Correlates Analysis of the mRNA-1273 COVID-19 Vaccine Efficacy Trial. *medRxiv*, 2021.2008.2009.21261290, doi:10.1101/2021.08.09.21261290 (2021).

3 Juno, J. A. *et al.* Humoral and circulating follicular helper T cell responses in recovered patients with COVID-19. *Nature medicine* **26**, 1428-1434, doi:10.1038/s41591-020-0995-0 (2020).

4 Koutsakos, M. *et al.* Integrated immune dynamics define correlates of COVID-19 severity and antibody responses. *Cell Rep Med* **2**, 100208, doi:10.1016/j.xcrm.2021.100208 (2021).

5 Rydyznski Moderbacher, C. *et al.* Antigen-Specific Adaptive Immunity to SARS-CoV-2 in Acute COVID-19 and Associations with Age and Disease Severity. *Cell*, doi:10.1016/j.cell.2020.09.038 (2020).

6 Zhang, J. *et al.* Spike-specific circulating T follicular helper cell and cross-neutralizing antibody responses in COVID-19-convalescent individuals. *Nature microbiology*, doi:10.1038/s41564-020-00824-5 (2020).

7 Lederer, K. *et al.* SARS-CoV-2 mRNA Vaccines Foster Potent Antigen-Specific Germinal Center Responses Associated with Neutralizing Antibody Generation. *Immunity*, doi:10.1016/j.immuni.2020.11.009 (2020).

8 Baumjohann, D. & Fazilleau, N. Antigen-dependent multistep differentiation of T-follicular helper cells and its role in SARS-CoV-2 infection and vaccination. *European journal of immunology*, doi:10.1002/eji.202049148 (2021).

9 Shaan Lakshmanappa, Y. *et al.* SARS-CoV-2 induces robust germinal center CD4 T follicular helper cell responses in rhesus macaques. *Nature communications* **12**, 541, doi:10.1038/s41467-020-20642-x (2021).

10 Painter, M. M. *et al.* Rapid induction of antigen-specific CD4⁺ T cells is associated with coordinated humoral and cellular immune responses to SARS-CoV-2 mRNA vaccination. *Immunity*, doi:10.1016/j.immuni.2021.08.001 (2021).

11 Dan, J. M. *et al.* Immunological memory to SARS-CoV-2 assessed for greater than six months after infection. *bioRxiv*, 2020.2011.2015.383323, doi:10.1101/2020.11.15.383323 (2020).

12 Grifoni, A. *et al.* Targets of T Cell Responses to SARS-CoV-2 Coronavirus in Humans with COVID-19 Disease and Unexposed Individuals. *Cell*, doi:10.1016/j.cell.2020.05.015 (2020).

13 Tauzin, A. *et al.* A single dose of the SARS-CoV-2 vaccine BNT162b2 elicits Fc-mediated antibody effector functions and T cell responses. *Cell Host Microbe* **29**, 1137-1150.e1136, doi:10.1016/j.chom.2021.06.001 (2021).

14 Dan, J. M. *et al.* Immunological memory to SARS-CoV-2 assessed for up to 8 months after infection. *Science (New York, N.Y.)* **371**, doi:10.1126/science.abf4063 (2021).

15 Goel, R. R. *et al.* mRNA Vaccination Induces Durable Immune Memory to SARS-CoV-2 with Continued Evolution to Variants of Concern. *bioRxiv*, 2021.2008.2023.457229, doi:10.1101/2021.08.23.457229 (2021).

16 Crotty, S. Hybrid immunity. *Science (New York, N.Y.)* **372**, 1392-1393, doi:10.1126/science.abj2258 (2021).

17 Prendecki, M. *et al.* Effect of previous SARS-CoV-2 infection on humoral and T-cell responses to single-dose BNT162b2 vaccine. *Lancet (London, England)* **397**, 1178-1181, doi:10.1016/s0140-6736(21)00502-x (2021).
18 Oberhardt, V. *et al.* Rapid and stable mobilization of CD8+ T cells by SARS-CoV-2 mRNA vaccine. *Nature*, doi:10.1038/s41586-021-03841-4 (2021).
19 Akondy, R. S. *et al.* Origin and differentiation of human memory CD8 T cells after vaccination. *Nature* **552**, 362-367, doi:10.1038/nature24633 (2017).
20 Long, H. M. *et al.* MHC II tetramers visualize human CD4+ T cell responses to Epstein-Barr virus infection and demonstrate atypical kinetics of the nuclear antigen EBNA1 response. *The Journal of experimental medicine* **210**, 933-949, doi:10.1084/jem.20121437 (2013).
21 Raziorrouh, B. *et al.* Virus-Specific CD4+ T Cells Have Functional and Phenotypic Characteristics of Follicular T-Helper Cells in Patients With Acute and Chronic HCV Infections. *Gastroenterology* **150**, 696-706.e693, doi:https://doi.org/10.1053/j.gastro.2015.11.005 (2016).
22 Wheatley, A. K. *et al.* Evolution of immune responses to SARS-CoV-2 in mild-moderate COVID-19. *Nature communications* **12**, 1162, doi:10.1038/s41467-021-21444-5 (2021).
23 Woldemeskel, B. A., Garliss, C. C. & Blankson, J. N. SARS-CoV-2 mRNA vaccines induce broad CD4+ T cell responses that recognize SARS-CoV-2 variants and HCoV-NL63. *The Journal of clinical investigation* **131**, doi:10.1172/jci149335 (2021).
24 Peng, Y. *et al.* Broad and strong memory CD4(+) and CD8(+) T cells induced by SARS-CoV-2 in UK convalescent individuals following COVID-19. *Nature immunology* **21**, 1336-1345, doi:10.1038/s41590-020-0782-6 (2020).
25 Tarke, A. *et al.* Comprehensive analysis of T cell immunodominance and immunoprevalence of SARS-CoV-2 epitopes in COVID-19 cases. *Cell Rep Med* **2**, 100204, doi:10.1016/j.xcrm.2021.100204 (2021).
26 Jensen, K. K. *et al.* Improved methods for predicting peptide binding affinity to MHC class II molecules. *Immunology* **154**, 394-406, doi:10.1111/imm.12889 (2018).
27 Mateus, J. *et al.* Selective and cross-reactive SARS-CoV-2 T cell epitopes in unexposed humans. *Science (New York, N.Y.)* **370**, 89-94, doi:10.1126/science.abd3871 (2020).
28 Loyal, L. *et al.* Cross-reactive CD4(+) T cells enhance SARS-CoV-2 immune responses upon infection and vaccination. *Science (New York, N.Y.)*, doi:10.1126/science.abh1823 (2021).
29 Cohen, K. W. *et al.* Longitudinal analysis shows durable and broad immune memory after SARS-CoV-2 infection with persisting antibody responses and memory B and T cells. *Cell Rep Med* **2**, 100354, doi:10.1016/j.xcrm.2021.100354 (2021).
30 Gong, F. *et al.* Peripheral CD4+ T cell subsets and antibody response in COVID-19 convalescent individuals. *The Journal of clinical investigation*, doi:10.1172/jci141054 (2020).
31 Bentebibel, S. E. *et al.* Induction of ICOS+CXCR3+CXCR5+ TH cells correlates with antibody responses to influenza vaccination. *Science translational medicine* **5**, 176ra132, doi:10.1126/scitranslmed.3005191 (2013).
32 Herati, R. S. *et al.* Successive annual influenza vaccination induces a recurrent oligoclonotypic memory response in circulating T follicular helper cells. *Science immunology* **2**, doi:10.1126/sciimmunol.aag2152 (2017).

33 Koutsakos, M. *et al.* Circulating T(FH) cells, serological memory, and tissue compartmentalization shape human influenza-specific B cell immunity. *Science translational medicine* **10**, doi:10.1126/scitranslmed.aan8405 (2018).
34 Hill, D. L. *et al.* Impaired HA-specific T follicular helper cell and antibody responses to influenza vaccination are linked to inflammation in humans. *medRxiv*, 2021.2004.2007.21255038, doi:10.1101/2021.04.07.21255038 (2021).
35 Huber, J. E. *et al.* Dynamic changes in circulating T follicular helper cell composition predict neutralising antibody responses after yellow fever vaccination. *Clinical & translational immunology* **9**, e1129, doi:10.1002/cti2.1129 (2020).
36 Chang, C. M. *et al.* Profiling of T Cell Repertoire in SARS-CoV-2-Infected COVID-19 Patients Between Mild Disease and Pneumonia. *Journal of clinical immunology* **41**, 1131-1145, doi:10.1007/s10875-021-01045-z (2021).
37 Dykema, A. G. *et al.* Functional characterization of CD4+ T-cell receptors cross-reactive for SARS-CoV-2 and endemic coronaviruses. *The Journal of clinical investigation*, doi:10.1172/jci146922 (2021).
38 Minervina, A. A. *et al.* Longitudinal high-throughput TCR repertoire profiling reveals the dynamics of T-cell memory formation after mild COVID-19 infection. *eLife* **10**, doi:10.7554/eLife.63502 (2021).
39 Nguyen, T. H. O. *et al.* CD8(+) T cells specific for an immunodominant SARS-CoV-2 nucleocapsid epitope display high naive precursor frequency and TCR promiscuity. *Immunity* **54**, 1066-1082.e1065, doi:10.1016/j.immuni.2021.04.009 (2021).
40 Painter, M. M. *et al.* Rapid induction of antigen-specific CD4⁺ T cells guides coordinated humoral and cellular immune responses to SARS-CoV-2 mRNA vaccination. *bioRxiv*, 2021.2004.2021.440862, doi:10.1101/2021.04.21.440862 (2021).
41 Ebinger, J. E. *et al.* Antibody responses to the BNT162b2 mRNA vaccine in individuals previously infected with SARS-CoV-2. *Nature medicine* **27**, 981-984, doi:10.1038/s41591-021-01325-6 (2021).
42 Saadat, S. *et al.* Binding and Neutralization Antibody Titers After a Single Vaccine Dose in Health Care Workers Previously Infected With SARS-CoV-2. *Jama* **325**, 1467-1469, doi:10.1001/jama.2021.3341 (2021).
43 Schulien, I. *et al.* Characterization of pre-existing and induced SARS-CoV-2-specific CD8(+) T cells. *Nature medicine* **27**, 78-85, doi:10.1038/s41591-020-01143-2 (2021).
44 Kared, H. *et al.* CD8+ T cell responses in convalescent COVID-19 individuals target epitopes from the entire SARS-CoV-2 proteome and show kinetics of early differentiation. *bioRxiv*, doi:10.1101/2020.10.08.330688 (2020).
45 Mudd, P. A. *et al.* SARS-CoV-2 mRNA vaccination elicits robust and persistent T follicular helper cell response in humans. *bioRxiv*, 2021.2009.2008.459485, doi:10.1101/2021.09.08.459485 (2021).
46 Yang, J. *et al.* CD4+ T cells recognize unique and conserved 2009 H1N1 influenza hemagglutinin epitopes after natural infection and vaccination. *International immunology* **25**, 447-457, doi:10.1093/intimm/dxt005 (2013).
47 Guvenel, A. *et al.* Epitope-specific airway-resident CD4+ T cell dynamics during experimental human RSV infection. *The Journal of clinical investigation* **130**, 523-538, doi:10.1172/JCI131696 (2020).
48 James, E. A. *et al.* Yellow fever vaccination elicits broad functional CD4+ T cell responses that recognize structural and nonstructural proteins. *Journal of virology* **87**, 12794-12804, doi:10.1128/jvi.01160-13 (2013).
49 Folegatti, P. M. *et al.* Safety and immunogenicity of the ChAdOx1 nCoV-19 vaccine against SARS-CoV-2: a preliminary report of a phase 1/2, single-blind, randomised

controlled trial. *Lancet (London, England)* **396**, 467-478, doi:10.1016/s0140-6736(20)31604-4 (2020).
50 Jergović, M. *et al.* Competent immune responses to SARS-CoV-2 variants in older adults following mRNA vaccination. *bioRxiv*, 2021.2007.2022.453287, doi:10.1101/2021.07.22.453287 (2021).
51 Dash, P., Wang, G. C. & Thomas, P. G. Single-Cell Analysis of T-Cell Receptor αβ Repertoire. *Methods in molecular biology (Clifton, N.J.)* **1343**, 181-197, doi:10.1007/978-1-4939-2963-4_15 (2015).
52 Lefranc, M. P. *et al.* IMGT®, the international ImMunoGeneTics information system® 25 years on. *Nucleic acids research* **43**, D413-422, doi:10.1093/nar/gku1056 (2015).
53 Gu, Z., Gu, L., Eils, R., Schlesner, M. & Brors, B. circlize Implements and enhances circular visualization in R. *Bioinformatics (Oxford, England)* **30**, 2811-2812, doi:10.1093/bioinformatics/btu393 (2014).

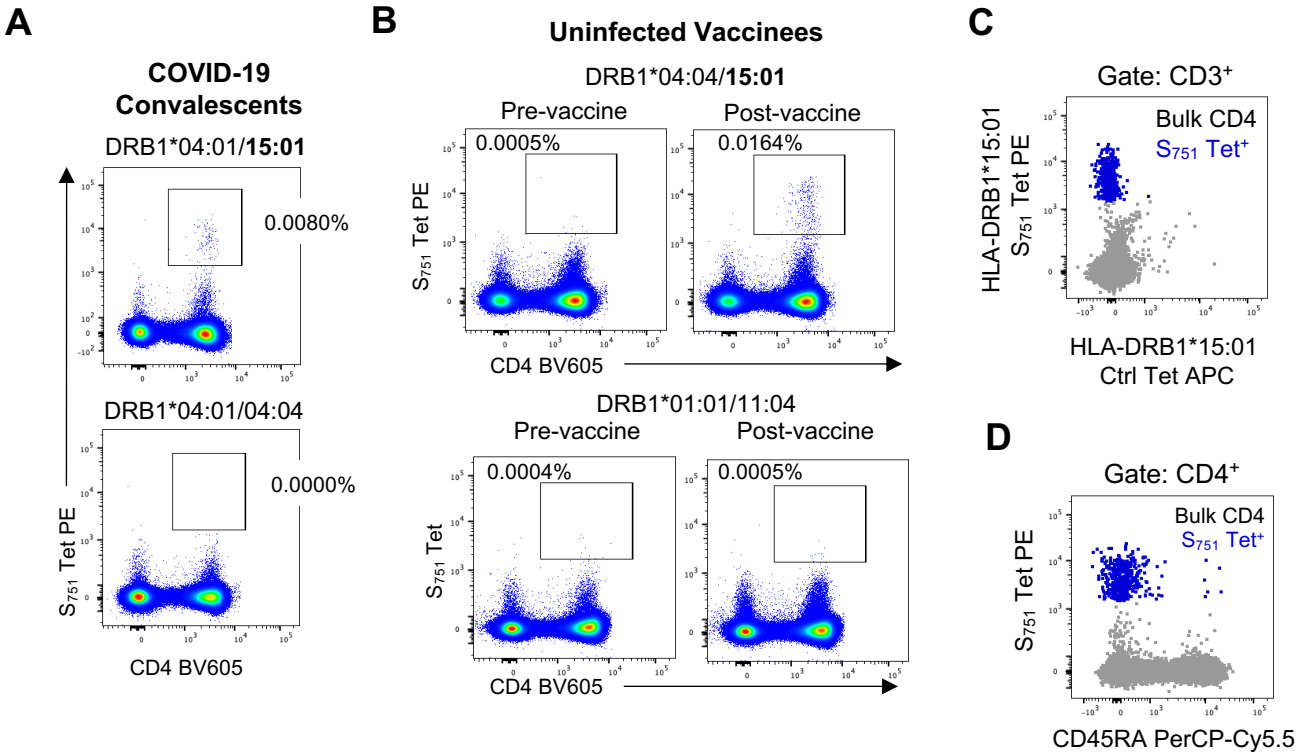

Figure 1. Specificity of HLA-DRB1*15:01/S_{751} tetramers. (A) Staining of HLA-DRB1*15:01/S_{751} tetramer on cryopreserved PBMC from individuals recovered from mild COVID-19 infection with or without the HLA-DRB1*15 allele. (B) Tetramer staining on PBMC collected prior to or after 2 doses of BNT162b2 vaccine in individuals with or without the HLA-DRB1*15 allele. (C) Co-staining of PBMC from a BNT162b2 vaccinated individual with HLA-DRB1*15:01 tetramers loaded with S_{751} or an irrelevant control peptide. (D) Co-staining of CD45RA and S_{751} tetramer following BNT162b2 vaccination.

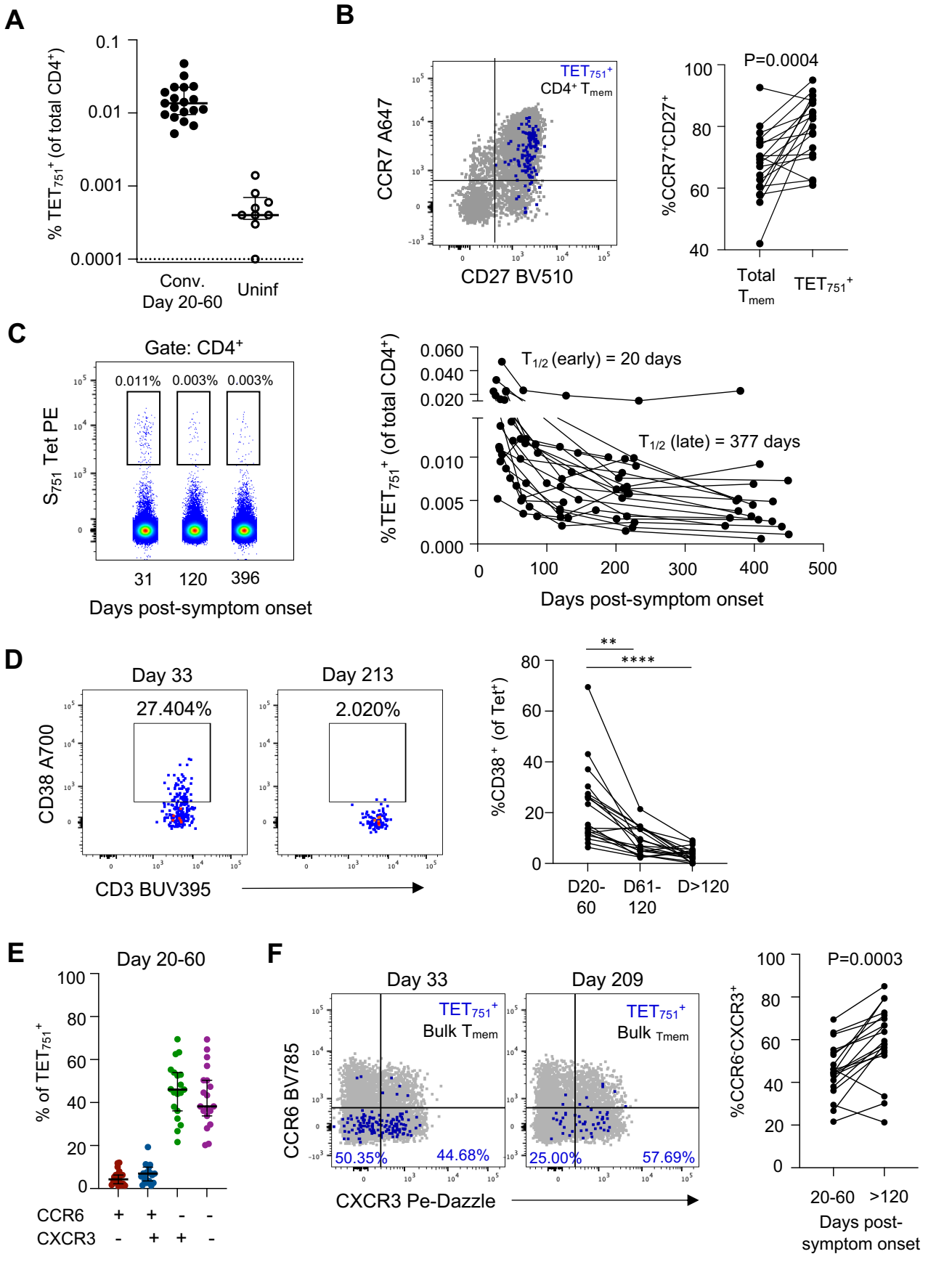

Figure 2. Establishment of S_{751}-specific CD4⁺ T cell memory following mild COVID-19. (A) Frequency of TET_{751}^+ cells (as % of total $CD4^+$) among uninfected (n=9) or COVID-19 convalescent individuals sampled 20 to 60 days post-symptom onset (n=19). (B) Representative plots demonstrating expression of CCR7 and CD27 on TET_{751}^+ or bulk T_{mem} (non-naïve $CD4^+$) subsets. Comparison of T_{CM} ($CCR7^+CD27^+$) phenotype between tet^+ or bulk T_{mem} assessed using Wilcoxon test (n=19). (C) Representative staining and frequencies of TET_{751}^+ cells over the course of 1 to 15 months post-symptom onset (n=21). (D) Expression of CD38 on TET_{751}^+ cells during longitudinal follow-up (n=19 at d20-60 and d>120; n=15 at d61-120). Statistics assessed by Kruskal-Wallis and Dunn's multiple comparisons test (**p<0.01, ****p<0.001). (E, F) Expression of CCR6 and CXCR3 on TET_{751}^+ or T_{mem} cells during (E) early or (F) late convalescence (n=19). Lines indicate median and IQR. Statistics assessed by Wilcoxon test.

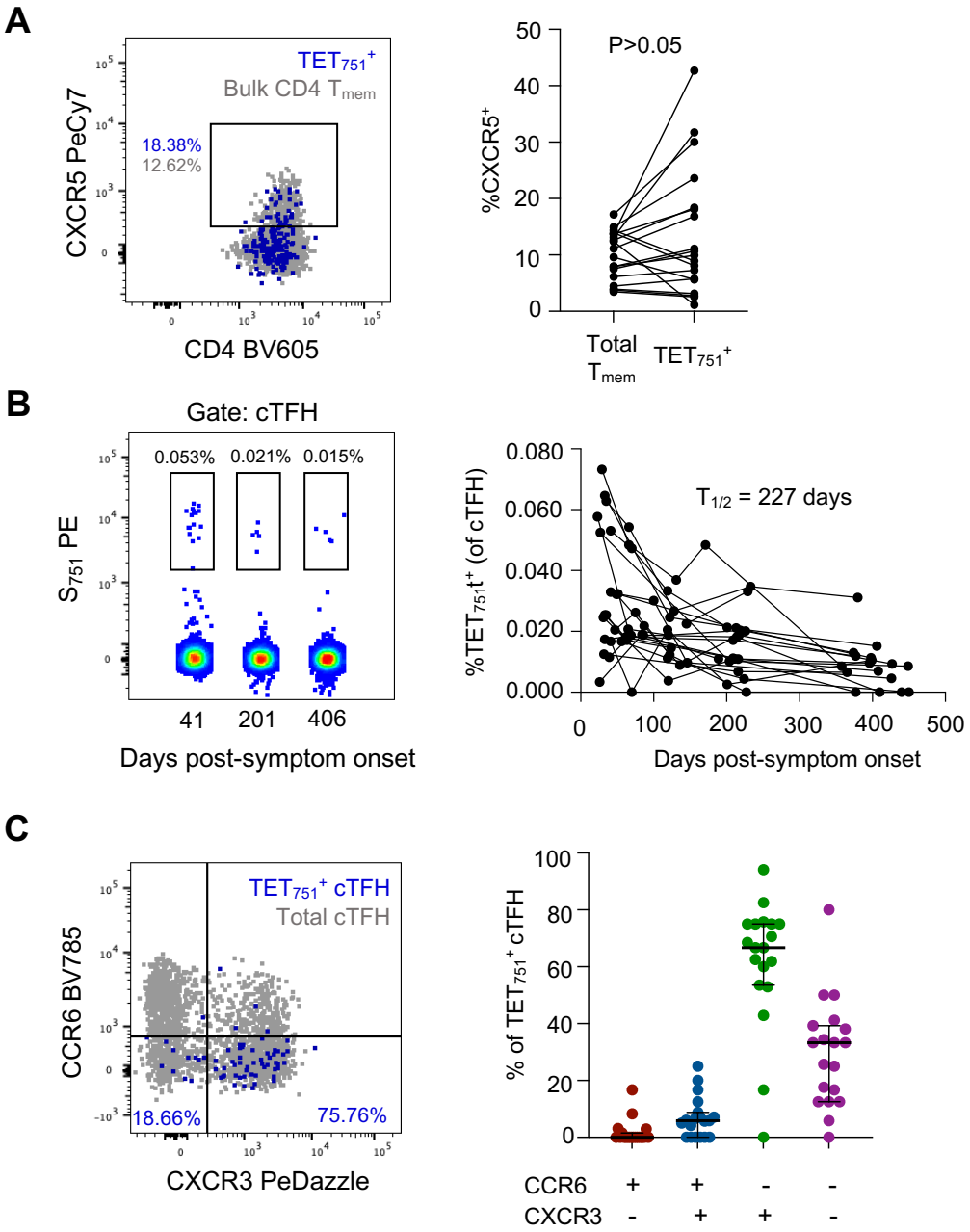

Figure 3. Frequency and phenotype of CXCR5⁺ S_{751}-specific cTFH. (A) Representative staining and frequency of CXCR5⁺ cells among CD4⁺ T_{mem} and TET_{751}^+ cells at days 20-60 post-symptom onset (n=19). Statistics assessed by Wilcoxon test. (B) Longitudinal analysis of the frequency of TET_{751}^+ cells among the cTFH (CXCR5⁺ T_{mem}) population (n=21). (C) Expression of CCR6 and CXCR3 among TET_{751}^+ (blue) or bulk (grey) cTFH at 20-60 days post-symptom onset (n=19). Graph indicates median and IQR.

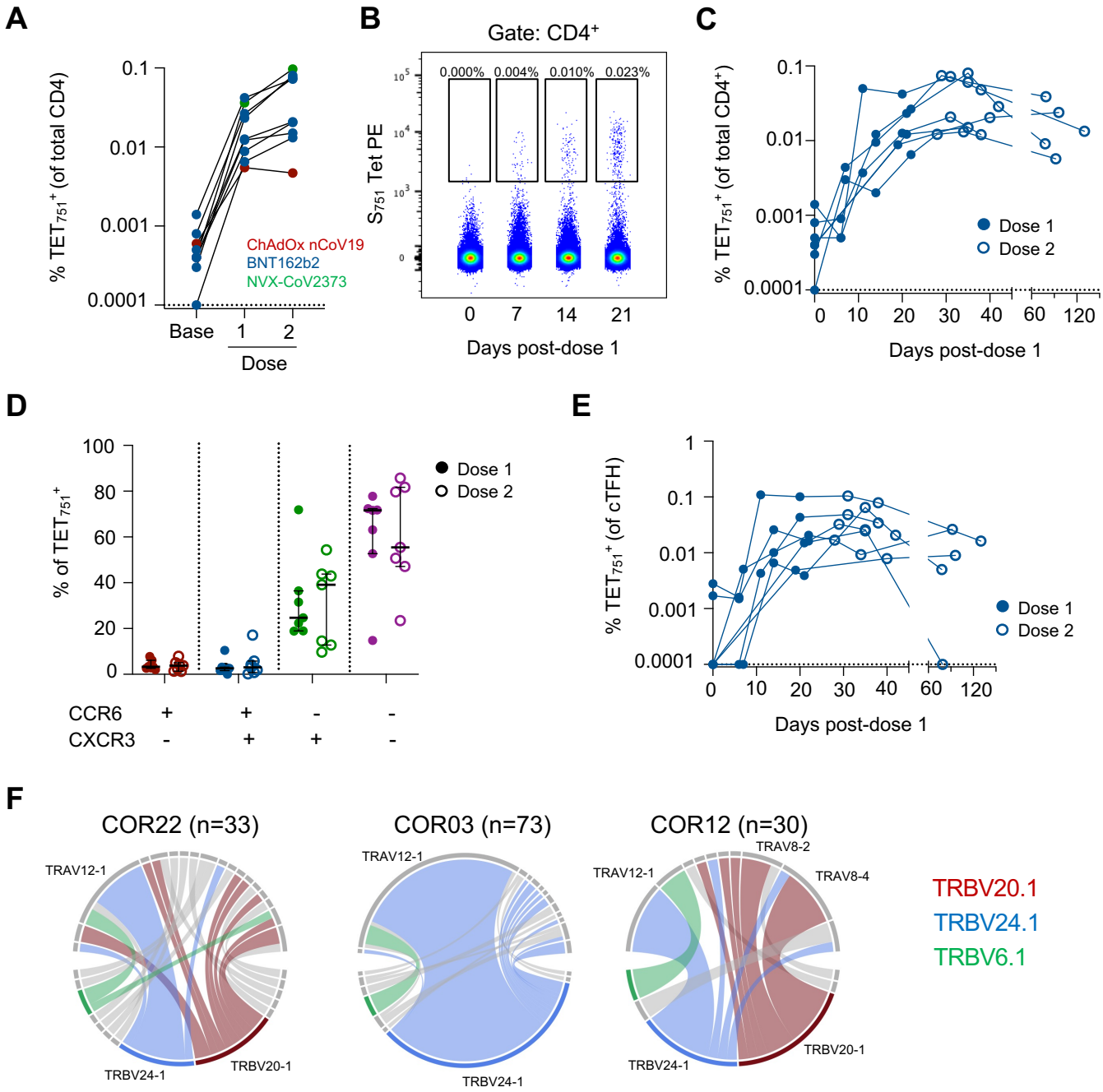

Figure 4. Induction of S_{751}-specific CD4 T cells following vaccination.
(A) Frequencies of S_{751}-specific T cells at baseline, week 3 post-dose 1, or week 2 post-dose 2 among 9 previously uninfected individuals. Blue, BNT162b2; red, ChAdOx-nCoV19; green, NVX-CoV2373. (B) Representative staining of S_{751} tetramer among $CD4^+$ T cells following immunization with one dose of BTN12b2 in a previously uninfected subject. (C) Longitudinal S_{751}-specific T cell frequencies at baseline and following BNT162b2 vaccination among 7 previously uninfected individuals. Closed circles, samples collected after dose 1; open circles, samples collected after dose 2. (D) CCR6 and CXCR3 expression on TET_{751}^+ cells at week 3 post-dose 1 or week 2 post-dose 2 among 7 individuals vaccinated with BNT162b2. (E) Longitudinal S_{751}-specific cTFH frequencies at baseline and following BNT162b2 vaccination among 7 previously uninfected individuals. Closed circles, samples collected after dose 1; open circles, samples collected after dose 2. (F) Circos plots indicating pairing of TRAV and TRBV genes among sorted TET_{751}^+ cells for three subjects after the second vaccine dose.

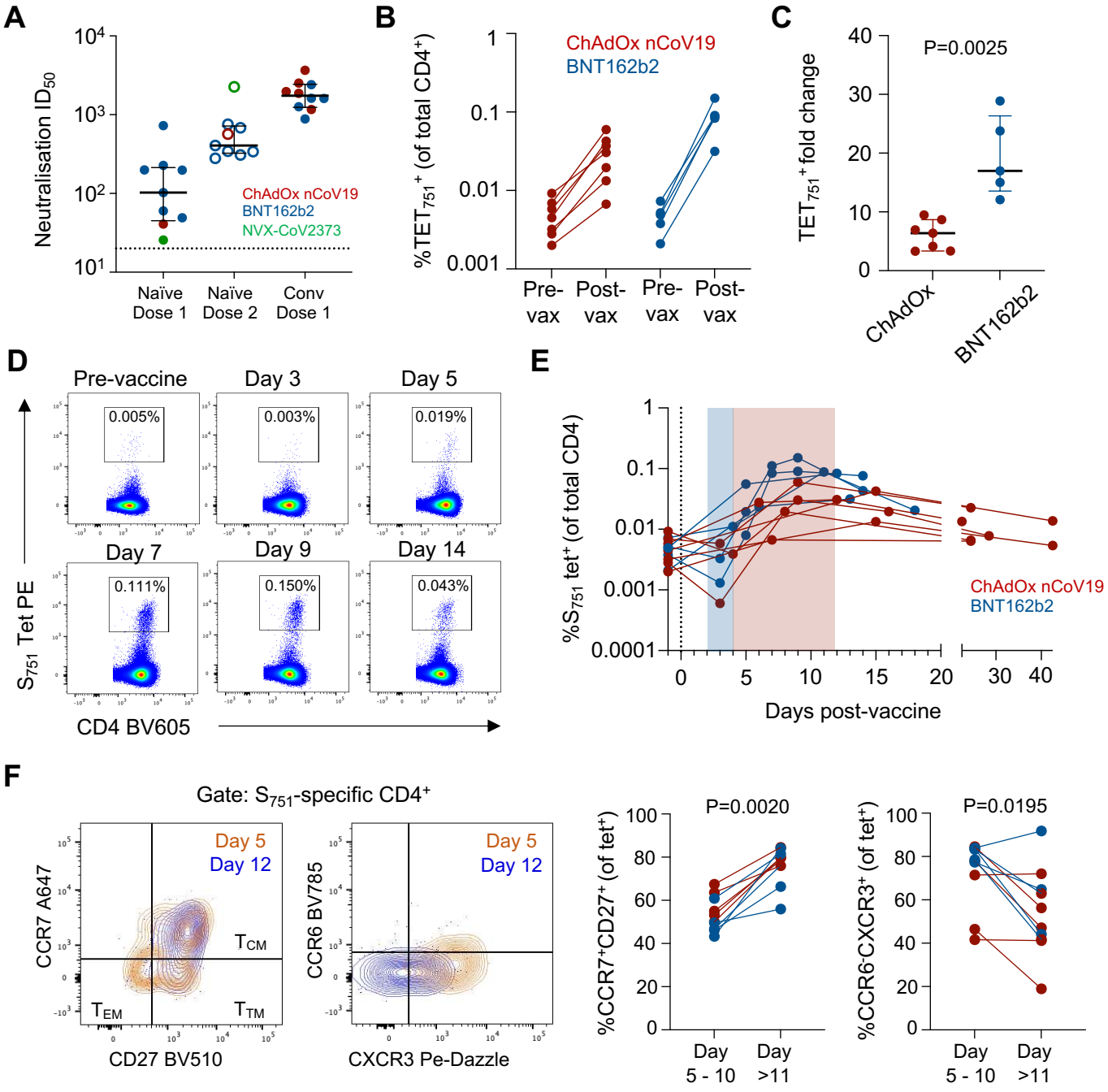

Figure 5. Recall of S_{751}-specific CD4⁺ T cells following vaccination of COVID-19 convalescent individuals. (A) Neutralising antibody titres against SARS-CoV-2 among the naïve vaccination cohort (3 weeks post-dose 1, or 3 weeks post-dose 2; n=9) and convalescent subjects (2 weeks post-dose 1, n=10). (B) Changes in TET_{751}^+ T cell frequency between pre-vaccine and post-vaccine (1-2 weeks post-dose 1) among convalescent subjects. (C) Fold change in TET_{751}^+ T cell frequencies according to vaccine platform. (D) Time course of S_{751}-specific T cell expansion in a single convalescent individual prior to and following a single dose of BNT162b2. (E) Longitudinal tetramer frequencies among 12 individuals (n=7 AstraZeneca, red; n=5 Pfizer/BioNTech, blue). Pre-vaccine samples are set at day -1. Blue shading indicates days 3-4 post-immunization, red indicates days 4-12. (F) Expression of CCR7/CD27 and CCR6/CXCR3 on TET_{751}^+ cells at early (days 5-10) or late (day >11) timepoints after vaccination. N=5 ChAdOx nCoV19, red; n=5 BNT162b2, blue; statistics assessed by Wilcoxon test.

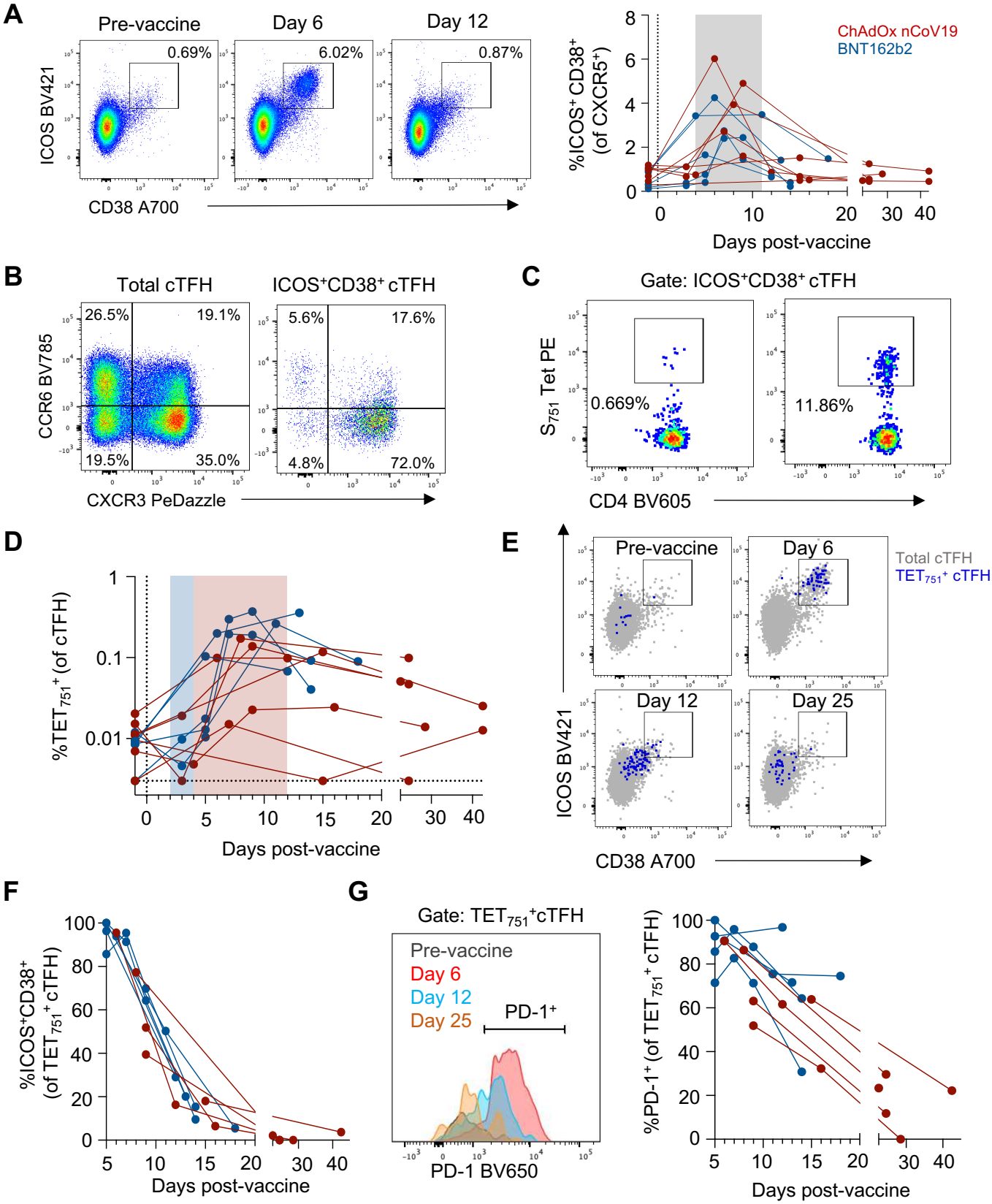

Figure 6. Vaccine-associated recall of activated and S_{751}-specific cTFH. (A) Representative staining and frequency of ICOS$^+$CD38$^+$ cTFH following single dose vaccination of convalescent subjects (n=12). Grey shading indicates days 4-11 post-vaccination. (B) Representative staining of CCR6 and CXCR3 on total cTFH (CD4$^+$CXCR5$^+$) or ICOS$^+$CD38$^+$ cTFH. Data are representative of 10 individuals with samples available from day 5-11 post-vaccination. (C) S_{751} tetramer binding within the ICOS$^+$CD38$^+$ cTFH population in two subjects with low (<1%) or high (>10%) S_{751}-specific frequencies. (D) Longitudinal S_{751}-specific cTFH frequencies among n=12 convalescent subjects following vaccination. Limit of detection, 0.003% (indicated by dashed line). (E) Expression of ICOS and CD38 on TET$_{751}^+$ cTFH (blue) in a single individual over time. (F) Proportion of S_{751}-specific cTFH with an activated (ICOS$^+$CD38$^+$) phenotype over time (n=10). (G) Expression of PD-1 on S_{751}-specific cTFH following vaccination (n=10).

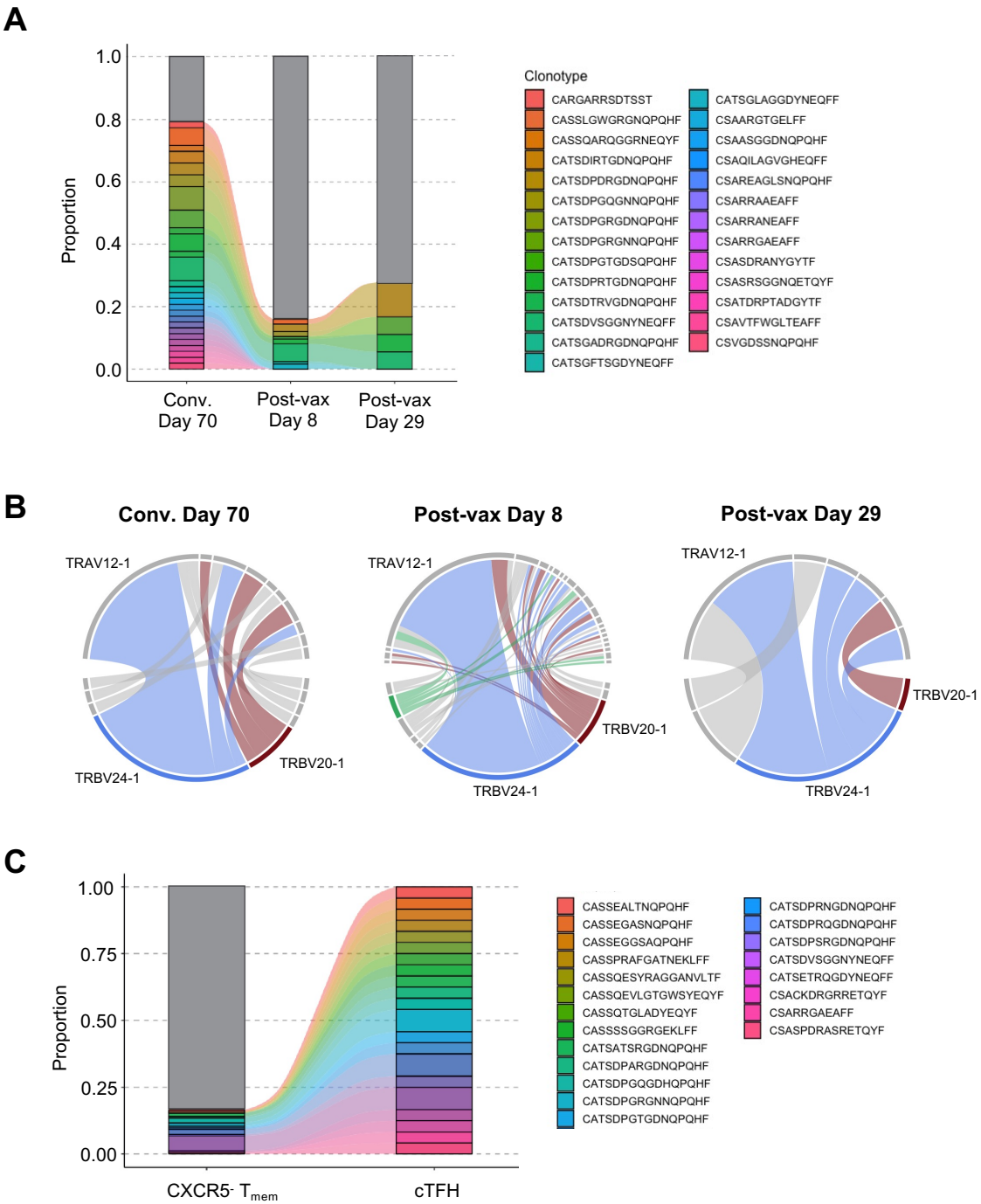

Figure 7. Longitudinal tracking of S_{751}-specific TCR clonotypes. (A) Persistence of TRBV clonotypes across three longitudinal samples in a single convalescent individual. Colours identify the 27 most frequent clonotypes comprising 80% of the recovered repertoire at the day 70 convalescent timepoint. (B) Circos plots indicating TRAV and TRBV pairing at each indicated timepoint. (C) Clonotype sharing between cTFH and $CXCR5^-$ T_{mem} across among cells recovered from any timepoint.

Supplemental Data

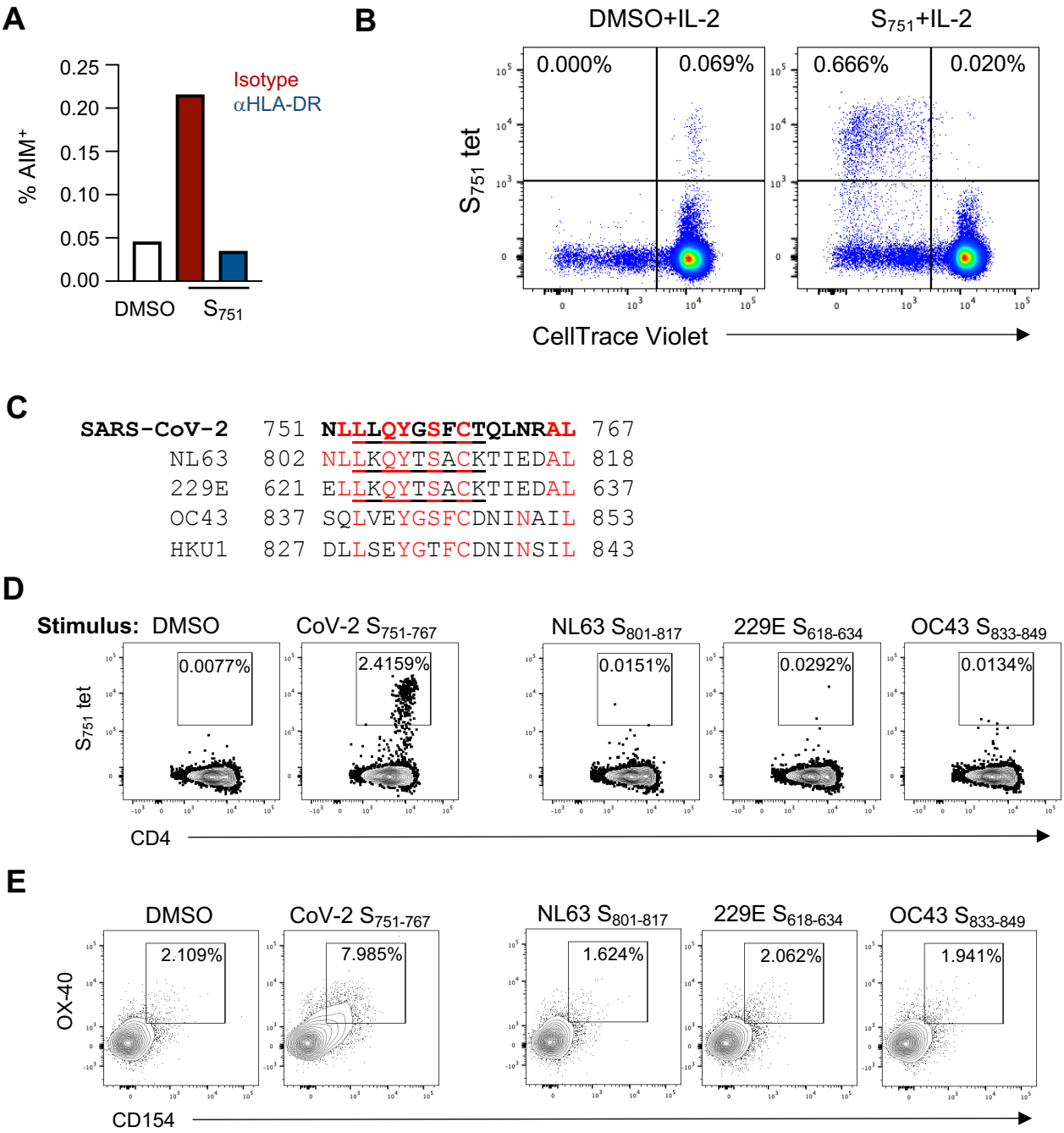

Supplemental Figure 1. HLA restriction of S_{751}-specific CD4 T cell responses and validation of HLA-DRB1*15/S_{751} tetramer staining. (A) Activation induced marker (AIM; $CD25^+OX\text{-}40^+$) $CD4^+$ T cell responses to S_{751} peptide (or DMSO control) stimulation in the presence or absence of anti-HLA-DR antibody. Results are representative of independent experiments across two different subjects. (B) In vitro expansion and proliferation of S_{751} tet^+ cells following 11 days of culture with IL-2 and S_{751} peptide or DMSO control. (C) Sequence alignment of SARS-CoV-2 $S_{751\text{-}767}$ sequence with hCoV NL63, 229E, OC43 and HKU1 spike proteins. Predicted core epitopes with strong binding to HLA-DRB1*15:01 according to NetMHCII 2.3 are underlined. (D) PBMC from HLA-DRB1*15:01 COVID-19 convalescent subjects following vaccination were stimulated with S_{751} peptide or analogous peptides from NL63, 229E or OC43 and IL-2 for 11 days, then stained with the DRB1*15:01/S_{751} tetramer. Results are representative of independent experiments in 3 subjects. (E) PBMC from HLA-DRB1*15:01 COVID-19 convalescent subjects following vaccination were stimulated with S_{751} peptide and IL-2 for 11 days to expand S_{751}-specific T cells and re-stimulated with S_{751} or analogous peptides from hCoV antigens to assess the antigen specificity of the *in vitro* expanded cells. Plots are gated on total $CD4^+$ T cells and show expression of OX-40 and CD154 (CD40L) following re-stimulation. Data are representative of experiments in two different individuals.

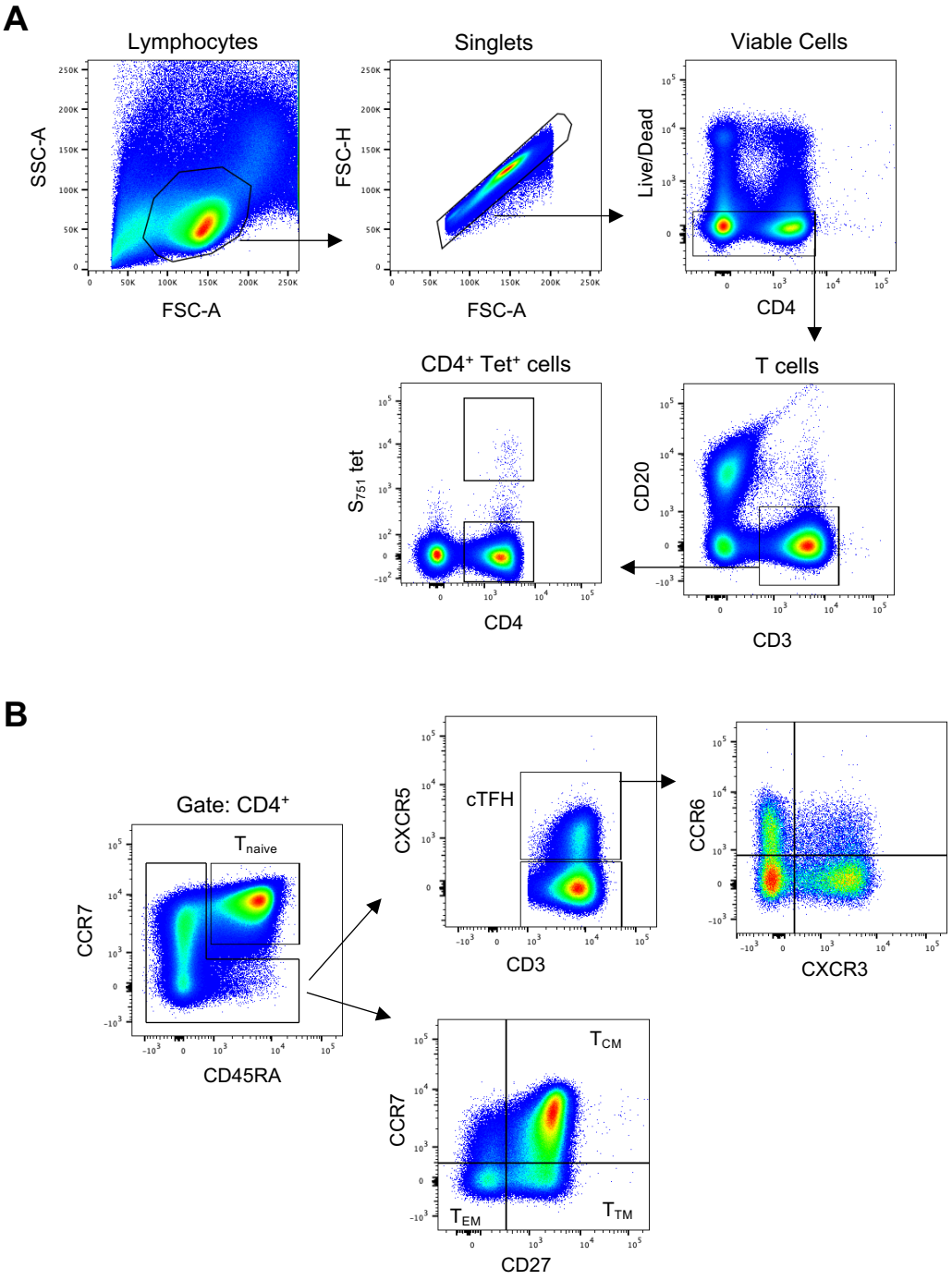

Supplemental Figure 2. Gating strategy for CD4⁺ T cell analysis
(A) Identification of lymphocytes, singlets, viable cells, $CD3^{+}CD20^{-}$ T cells, and gating for S751 tet^{+} $CD4^{+}$ cells. (B) Gating strategy for $CD4^{+}$ T cell subsets, including naïve versus memory cells, central/transitional/effector memory subsets, circulating T follicular helper cells, and CCR6/CXCR3 expression.

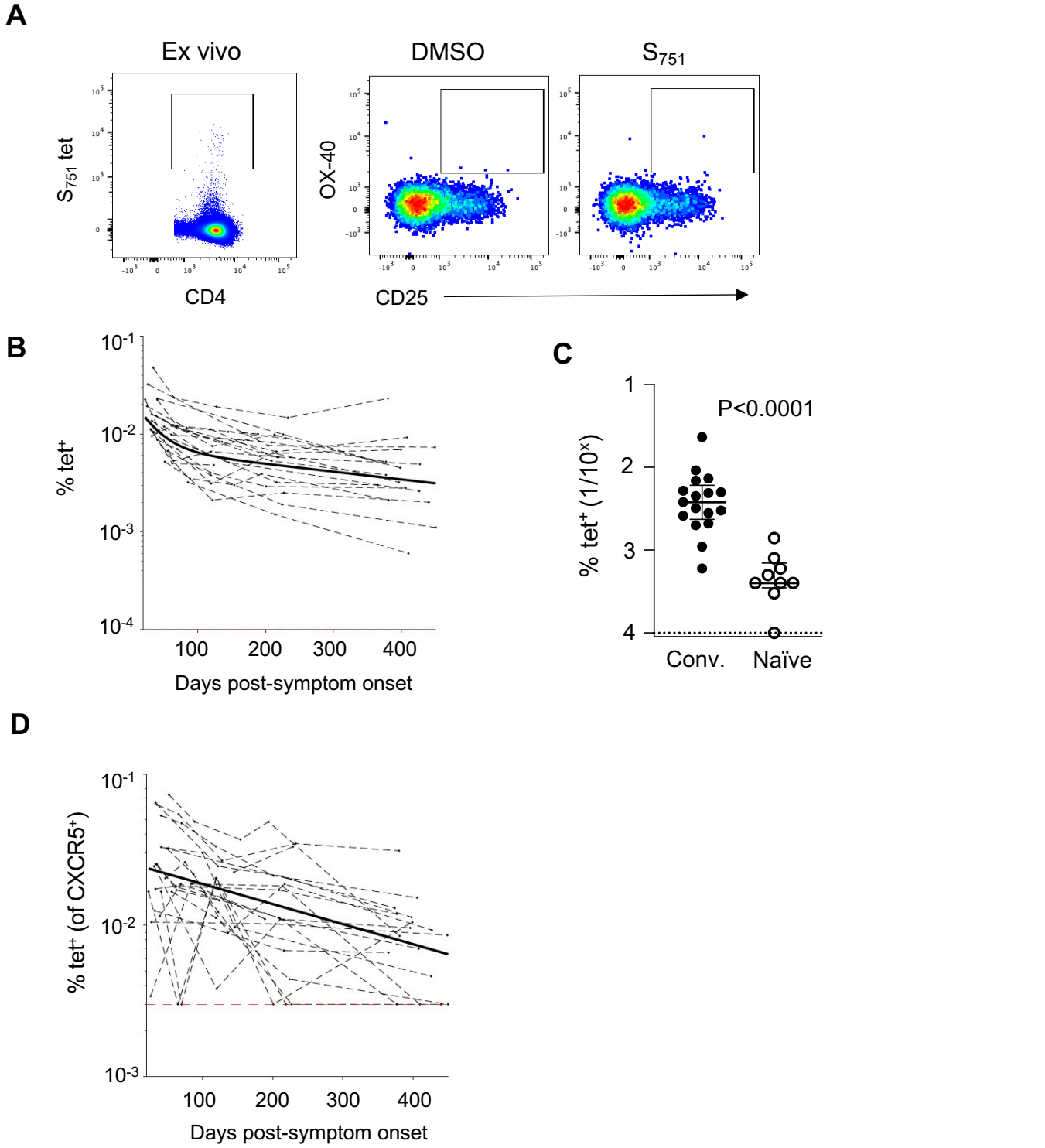

Supplemental Figure 3. Longitudinal S_{751}-specific T cell frequency and phenotype during convalescence. (A) *Ex vivo* S_{751} tetramer staining in a convalescent individual and paired AIM assay CD25/OX-40 staining following stimulation with S_{751} peptide. (B) Non-linear mixed effects model of TET_{751}^+ T cell decay. The limit of detection was fixed to 0.0001%. (C) Comparison of the frequency of S_{751} tet^+ cells at 365-450 days post-symptom onset among HLA-DRB1*15:01/02 convalescent donors (n=17) compared to HLA-DRB1*15:01/02 uninfected controls (n=9). Statistics assessed by Mann-Whitney test. (D) Non-linear mixed effects model of TET_{751}^+ cTFH decay. The limit of detection was fixed to 0.003%.

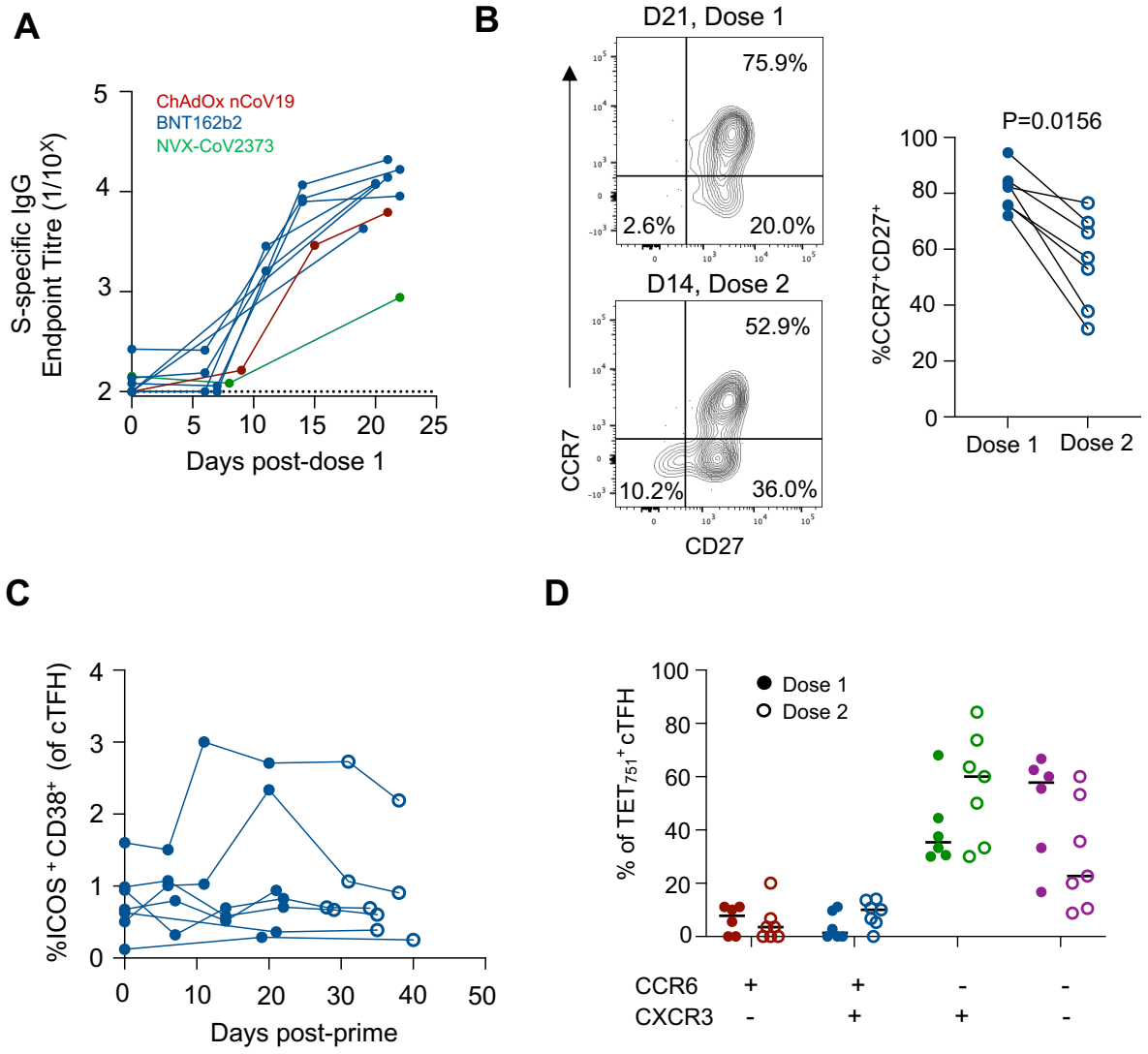

Supplemental Figure 4. Cellular and serological responses to vaccination among previously uninfected subjects. (A) Kinetics of anti-spike IgG titres after vaccine dose 1 (n=9). (B) CCR7 and CD27 expression on TET_{751}^{+} T cells at three weeks post-dose 1 or two weeks post-dose 2 in the BNT162b2 cohort (n=7). Statistics assessed by Wilcoxon test. (C) Longitudinal frequency of total activated ($ICOS^{+}CD38^{+}$) cTFH following BNT162b2 vaccination (n=7). Closed circles, samples after dose 1; open circles, samples after dose 2. (D) Phenotype of TET_{751}^{+} cTFH at three weeks post-dose 1 or one week post-dose 2 among the BNT162b2 cohort (n=7).

TRBV 20.1		Subjects	Common TRAV
	Public CSARRGTEAFF	COR12 COR22	TRAV8-2 TRAV8-4
	Private CSARRAAEAFF CSARRANEAFF CSARRGAEAFF CSARRGVEAFF CSATQGGELFF CSATRGGEQFF		
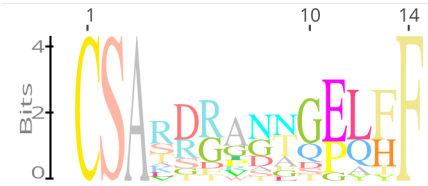	Public CSARDRANTGELFF	COR12 COR22	TRAV13-1
	Private CSARDRANAGELFF CSARGTRAFGEQYF CSASRGAGGGELFF CSATDRVNTGELFF		
TRBV 24.1			
	Public CATSDPRQGDNQPQHF	COR03 COR22	TRAV12-1
	CATSDPRVGDNQPQHF	COR03 COR12	TRAV12-1
	Private CATSATSRGDNQPQHF CATSDPGAGDIQPQHF CATSDPGRGSNQPQHF CATSDPRNGDNQPQHF CATSDPRQGDYQPQHF		
TRBV 6.1			
	Public CASSEGASNQPQHF	COR03 COR12 COR22	TRAV12-1
	Private CASSEGGSAQPQHF CASSEALTNQPQHF CASSEGASRQPQHF		

Supplemental Figure 5. Public and private TRBV clonotypes from TET_{751}^{+} T cells. TRBV sequences derived from TET_{751}^{+} T cells across three previously uninfected vaccinees. Conserved sequence motifs and associated private and public (shared among at least two subjects) clonotypes are indicated.

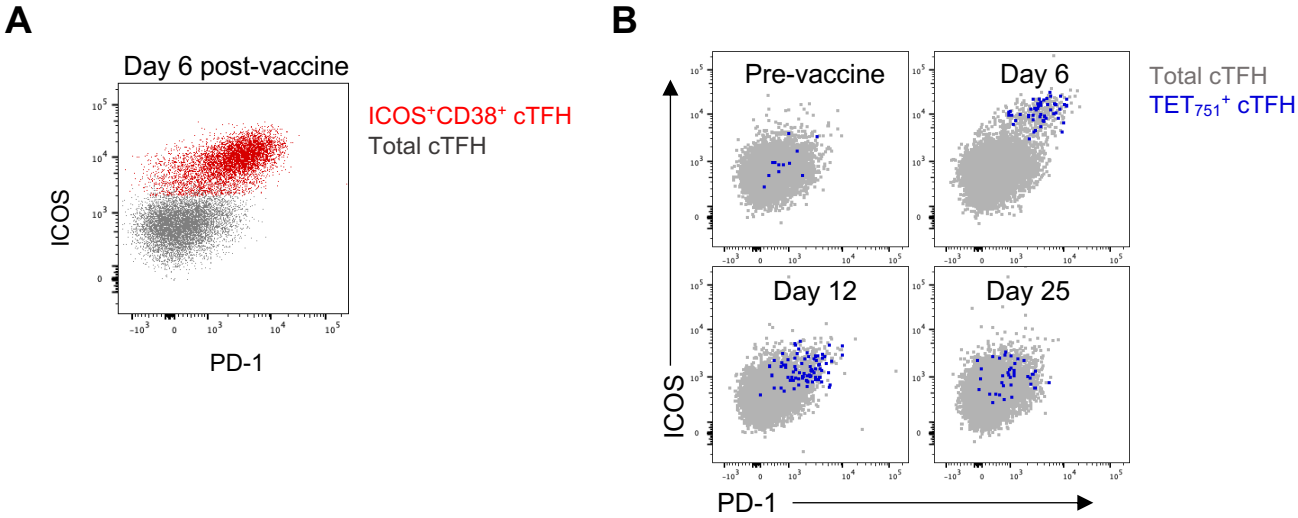

Supplemental Figure 6. Co-expression of CD38, ICOS and PD-1 on activated cTFH. (A) Representative staining of PD-1 expression on $ICOS^+CD38^+$ cTFH in a convalescent subject post-vaccination. (B) ICOS and PD-1 co-expression on TET_{751}^+ cTFH (blue) compared to total cTFH (grey) prior to and following vaccination.